Aligning Optimization Trajectories with Diffusion Models for Constrained Design Generation

Giorgio Giannone
Massachusetts Institute of Technology
Technical University of Denmark
ggiorgio@mit.edu

Akash Srivastava
MIT-IBM Watson AI Lab
akashsri@mit.edu

Ole Winther
Technical University of Denmark
University of Copenhagen
olwi@dtu.dk

Faez Ahmed
Massachusetts Institute of Technology
faez@mit.edu

Abstract

Generative models have had a profound impact on vision and language, paving the way for a new era of multimodal generative applications. While these successes have inspired researchers to explore using generative models in science and engineering to accelerate the design process and reduce the reliance on iterative optimization, challenges remain. Specifically, engineering optimization methods based on physics still outperform generative models when dealing with constrained environments where data is scarce and precision is paramount. To address these challenges, we introduce Diffusion Optimization Models (DOM) and Trajectory Alignment (TA), a learning framework that demonstrates the efficacy of aligning the sampling trajectory of diffusion models with the optimization trajectory derived from traditional physics-based methods. This alignment ensures that the sampling process remains firmly grounded in the underlying physical principles. Our method allows for generating feasible and high-performance designs in as few as two steps without the need for expensive preprocessing, external surrogate models, or additional labeled data. DOM also integrates an efficient conditioning approximation to speed up inference and a few steps of direct optimization to guide the process explicitly toward regions with superior manufacturability and performance. We apply our framework to structural topology optimization, a fundamental problem in mechanical design, evaluating its performance on in- and out-of-distribution configurations. Our results demonstrate that Trajectory Alignment outperforms state-of-the-art deep generative models on in-distribution configurations and halves the inference computational cost. When coupled with a few steps of optimization, it also improves manufacturability for out-of-distribution conditions. DOM shows the effectiveness of combining learning and optimization trajectories. By significantly improving engineering performance and inference efficiency, it enables us to generate high-quality designs in just a few steps and guide them toward regions of high performance and manufacturability, paving the way for the widespread application of generative models in large-scale data-driven design.

1 Introduction

The advancements in large vision [27, 20, 43, 85] and language [30, 21, 78] models have dramatically increased our capacity to process unstructured data, catalyzing a new era of multimodal and semantic

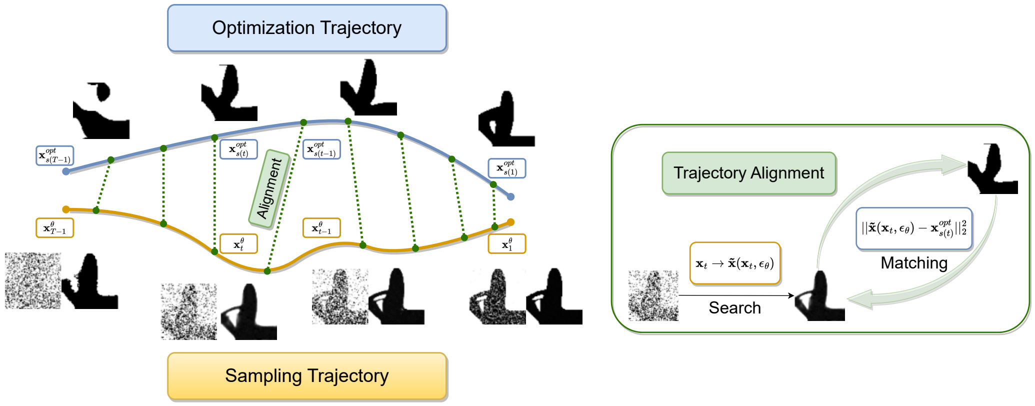
Optimization Trajectory
$\mathbf{x}^{opt}_{s(T-1)}$
$\mathbf{x}^{opt}_{s(t)}$
Alignment
$\mathbf{x}^{opt}_{s(t-1)}$
$\mathbf{x}^{opt}_{s(1)}$
$\mathbf{x}^{\theta}_{T-1}$
$\mathbf{x}^{\theta}_{t}$
$\mathbf{x}^{\theta}_{t-1}$
$\mathbf{x}^{\theta}_{1}$
Sampling Trajectory
Trajectory Alignment
$||\tilde{\mathbf{x}}(\mathbf{x}_t, \epsilon_\theta) - \mathbf{x}^{opt}_{s(t)}||^2_2$
Matching
$\mathbf{x}_t \rightarrow \tilde{\mathbf{x}}(\mathbf{x}_t, \epsilon_\theta)$
Search

(a) Sampling and Optimization Trajectory **(b)** Trajectory Alignment

Figure 1: Trajectory Alignment. Intermediate sampling steps in a Diffusion Optimization Model are matched with intermediate optimization steps. In doing so, the sampling path is biased toward the optimization path, guiding the data-driven path toward physical trajectories. This leads to significantly more precise samples.

generation [79, 67, 18, 80]. Inspired by this success, Deep Generative Models (DGMs) have been leveraged in the scientific [51, 61] and engineering field [84, 101], particularly for constraint-bound problems such as structural Topology Optimization (TO [95]), to expedite the design process.

Engineering designs predominantly rely on *iterative* optimization algorithms that discretize physical and chemical phenomena and iteratively improve design performance while meeting a set of constraint requirements. For instance, topology optimization aims to determine the optimal material distribution within a given design space, under specified loads and boundary conditions, to achieve the best performance according to a set of defined criteria, such as minimum weight or maximum stiffness. While iterative topology optimization methods, such as SIMP [15], hold great benefits, they face significant challenges in practical applications, especially for large-scale problems, owing to their computational complexity.

Recent advancements have sought to address these challenges by venturing into learning-based approaches for topology optimization, specifically deep generative models. These models are often trained on a dataset of optimal solutions under different constraints, to expedite or replace the optimization process and foster greater diversity in structural topologies by leveraging extensive datasets of pre-existing designs. This capacity to generate diverse solutions, coupled with the ability to consider multiple design variables, constraints, and objectives, makes learning-based methods particularly appealing in engineering design scenarios.

However, purely data-driven approaches to generative design tend to underperform compared to optimization-based methods. These methods typically focus on metrics like reconstruction quality, which often insufficiently capture the degree to which the engineering specifications are satisfied. The lack of physical information in data-driven methods and the absence of mechanisms to include iterative optimization details during the inference stage limit their effectiveness. This deficiency can limit the quality of the solutions generated, especially for problems with complex constraints and performance requirements. Therefore, there is a need for methods that combine data-driven and physics-based approaches to better address engineering challenges. To this end, structured generative models have shown great promise in generative topology optimization by leveraging techniques such as TopologyGANs [69] and TopoDiff [62].

Limitations. Despite these recent advances, structured generative models for engineering designs have several outstanding limitations that need to be addressed. For instance, these models often require additional supervised training data to learn guidance mechanisms that can improve performance and manufacturability [84]. In the case of Diffusion Models [43], we also have to run the forward models tens or hundreds of times to obtain a suitable topology [62]. Additionally, to condition the models on physical information, expensive FEA (Finite Element Analysis) preprocessing is required at both training and inference time to compute stress and energy fields [62, 69]. As a result, the sampling process is slow, and the inference process is computationally expensive, making it challenging to generalize and scale these methods effectively. This partially invalidates the advantages of data-driven approaches in terms of fast sampling and cheap design candidate generation.

Proposed Solution. We propose a conditional diffusion model that integrates data-driven and optimization-based methods to learn constrained problems and generate candidates in the engineering design domains (see Fig. 3). Instead of relying on computationally heavy physics-based exact solutions using FEM, our method employs cost-effective physics-informed approximations to manage sparsity in conditioning constraints. We introduce a Trajectory Alignment (TA) mechanism in the training phase that allows the model to leverage the information in the physical trajectory that was used by the optimization-based solution in the training data, drastically cutting down the sampling steps required for a topology. Our framework allows for further enhancing performance and manufacturability in complex situations by integrating a few stages of direct optimization. Our approach significantly reduces computational costs without sacrificing accuracy or effectiveness and can be easily adapted to novel design problems. By bridging the gap between generative modeling and engineering design, our proposed framework provides an efficient and effective solution for solving complex engineering problems. Intuitively, we show that diffusion models benefit greatly in precision metrics by learning from the trajectory taken by optimization methods represented by intermediate solutions and not just their final outcome.

Contribution. Our contributions are the following:

(i) We introduce the *Diffusion Optimization Models* (DOM), a versatile and efficient approach to incorporate performance awareness in generative models of engineering design problems while respecting constraints. The primary objective of DOM is to generate high-quality candidates rapidly and inexpensively, with a focus on topology optimization (TO) problems. DOM consists of

- *Trajectory Alignment* (TA) leverages iterative optimization and hierarchical sampling to match paths, distilling the optimizer knowledge in the sampling process. Doing so, DOM achieves high performance without the need for FEM solvers or guidance and can sample high-quality configurations in as few as two steps.
- *Dense Kernel Relaxation*, an efficient mechanism to relieve inference from expensive FEM pre-processing and
- *Few-Steps Direct Optimization* that improves manufacturability using a few optimization steps.

(ii) We perform extensive quantitative and qualitative evaluation in- and out-of-distribution, showing how kernel relaxation and trajectory alignment are both necessary for good performance and fast, cheap sampling. We also release a large, *multi-fidelity dataset* of sub-optimal and optimal topologies obtained by solving minimum compliance optimization problems. This dataset contains low-resolution (64x64), high-resolution (256x256), optimal (120k), and suboptimal (600K) topologies. To our knowledge, this is the first large-scale dataset of optimized designs providing intermediate suboptimal iterations.

2 Background

Here we briefly introduce the Topology Optimization problem [14], diffusion models [105, 44, 98], a class of deep generative models, conditioning and guidance mechanisms for diffusion models, and deep generative models for topology optimization [69, 62].

The Topology Optimization Problem. Topology optimization is a computational design approach that aims to determine the optimal arrangement of a structure, taking into account a set of constraints. Its objective is to identify the most efficient utilization of material while ensuring the structure meets specific performance requirements. One widely used method in topology optimization is the Solid Isotropic Material with Penalization (SIMP) method [13]. The SIMP method employs a density field to model the material properties, where the density indicates the proportion of material present in a particular region. The optimization process involves iteratively adjusting the density field, considering

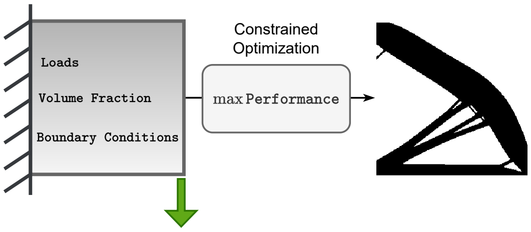

Figure 2: In topology optimization, the objective is to find the design with minimum compliance under given loads, boundary conditions, and volume fractions.

constraints such as stress or deformation. In the context of a mechanical system, a common objective is to solve a generic minimum compliance problem. This problem aims to find the distribution of material density, represented as $\mathbf{x} \in \mathbb{R}^n$, that minimizes the deformation of the structure under prescribed boundary conditions and loads [59]. Given a set of design variables $\mathbf{x} = \{\mathbf{x}_i\}_{i=0}^n$, where n is the domain dimensionality, the minimum compliance problems can be written as:

$$\begin{aligned} \min_{\mathbf{x}} \quad & c(\mathbf{x}) = F^T U(\mathbf{x}) \\ \text{s.t.} \quad & v(\mathbf{x}) = v^T \mathbf{x} < \bar{v} \\ & 0 \leq \mathbf{x} \leq 1 \end{aligned} \tag{1}$$

The goal is to find the design variables that minimize compliance $c(\mathbf{x})$ given the constraints. F is the tensor of applied loads and $U(\mathbf{x})$ is the node displacement, solution of the equilibrium equation $K(\mathbf{x})U(\mathbf{x}) = F$ where $K(\mathbf{x})$ is the stiffness matrix and is a function of the considered material. $v(\mathbf{x})$ is the required volume fraction. The problem is a relaxation of the topology optimization task, where the design variables are continuous between 0 and 1. One significant advantage of topology optimization is its ability to create optimized structures that meet specific performance requirements. However, a major drawback of topology optimization is that it can be computationally intensive and may require significant computational resources. Additionally, some approaches to topology optimization may be limited in their ability to generate highly complex geometries and get stuck in local minima.

Diffusion Models. Let $\mathbf{x}_0$ denote the observed data $\mathbf{x}_0 \in \mathbb{R}^D$. Let $\mathbf{x}_1, ..., \mathbf{x}_T$ denote T latent variables in $\mathbb{R}^D$. We now introduce, the *forward or diffusion process* q, the *reverse or generative process* p_θ, and the objective L. The forward or diffusion process q is defined as [44]: $q(\mathbf{x}_{1:T}|\mathbf{x}_0) = q(\mathbf{x}_1|\mathbf{x}_0) \prod_{t=2}^T q(\mathbf{x}_t|\mathbf{x}_{t-1})$. The beta schedule $\beta_1, \beta_2, ..., \beta_T$ is chosen such that the final latent image $\mathbf{x}_T$ is nearly Gaussian noise. The generative or inverse process p_θ is defined as: $p_\theta(\mathbf{x}_0, \mathbf{x}_{1:T}) = p_\theta(\mathbf{x}_0|\mathbf{x}_1)p(\mathbf{x}_T) \prod_{t=2}^T p_\theta(\mathbf{x}_{t-1}|\mathbf{x}_t)$. The neural network $\mu_\theta(\mathbf{x}_t, t)$ is shared among all time steps and is conditioned on t. The model is trained with a re-weighted version of the ELBO that relates to denoising score matching [105]. The negative ELBO L can be written as:

$$\mathbb{E}_q \left[-\log \frac{p_\theta(\mathbf{x}_0, \mathbf{x}_{1:T})}{q(\mathbf{x}_{1:T}|\mathbf{x}_0)} \right] = L_0 + \sum_{t=2}^T L_{t-1} + L_T, \tag{2}$$

where $L_0 = \mathbb{E}_{q(\mathbf{x}_1|\mathbf{x}_0)} [-\log p(\mathbf{x}_0|\mathbf{x}_1)]$ is the likelihood term (parameterized by a discretized Gaussian distribution) and, if $\beta_1, ...\beta_T$ are fixed, $L_T = \mathbb{KL}[q(\mathbf{x}_T|\mathbf{x}_0), p(\mathbf{x}_T)]$ is a constant. The terms L_{t-1} for $t = 2, ..., T$ can be written as: $L_{t-1} = \mathbb{E}_{q(\mathbf{x}_t|\mathbf{x}_0)} \Big[\mathbb{KL}[q(\mathbf{x}_{t-1}|\mathbf{x}_t, \mathbf{x}_0) \mid p(\mathbf{x}_{t-1}|\mathbf{x}_t)] \Big]$. The terms $L_{1:T-1}$ can be rewritten as a prediction of the noise ϵ added to $\mathbf{x}$ in $q(\mathbf{x}_t|\mathbf{x}_0)$. Parameterizing μ_θ using the noise prediction ϵ_θ, we can write

$$L_{t-1,\epsilon}(\mathbf{x}) = \mathbb{E}_{q(\epsilon)} \left[w_t \|\epsilon_\theta(\mathbf{x}_t(\mathbf{x}_0, \epsilon)) - \epsilon\|_2^2 \right], \tag{3}$$

where $w_t = \frac{\beta_t^2}{2\sigma_t^2 \alpha_t (1-\bar{\alpha}_t)}$, which corresponds to the ELBO objective [50, 56].

Conditioning and Guidance. Conditional diffusion models have been adapted for constrained engineering problems with performance requirements. TopoDiff [62] proposes to condition on loads, volume fraction, and physical fields similarly to [69] to learn a constrained generative model. In particular, the generative model can be written as:

$$p_\theta(\mathbf{x}_{t-1}|\mathbf{x}_t, \mathbf{c}, \mathbf{g}) = \mathcal{N}(\mathbf{x}_{t-1}; \mu_\theta(\mathbf{x}_t, \mathbf{c}) + \sum_{p=1}^P \mathbf{g}_p, \ \gamma), \tag{4}$$

where $\mathbf{c}$ is a conditioning term and is a function of the loads l, volume fraction v, and fields f, i.e $\mathbf{c} = h(l, v, f)$. The fields considered are the Von Mises stress $\sigma_{vm} = \sqrt{\sigma_{11}^2 - \sigma_{11}\sigma_{22} + \sigma_{22}^2 + 3\sigma_{12}^2}$ and the strain energy density field $W = (\sigma_{11}\epsilon_{11} + \sigma_{22}\epsilon_{22} + 2\sigma_{12}\epsilon_{12})/2$. Here σ_{ij} and ϵ_{ij} are the stress and energy components over the domain. $\mathbf{g}$ is a guidance term, containing information to guide the sampling process toward regions with low floating material (using a classifier and $\mathbf{g}_{fm}$) and regions with low compliance error, where the generated topologies are close to optimized one (using a regression model and $\mathbf{g}_c$). Where conditioning $\mathbf{c}$ is always present and applied during training, the guidance mechanism $\mathbf{g}$ is optional and applied only at inference time.

TopoDiff Limitations. TopoDiff is effective at generating topologies that fulfill the constraints and have low compliance errors. However, the generative model is expensive in terms of sampling time, because we need to sample tens or hundreds of layers for each sample. Additionally, given the model conditions on the Von Mises stress and the strain energy density, for each configuration of loads and boundary conditions, we have to preprocess the given configurations running a FEM solver. This, other than being computationally expensive and time-consuming, relies on fine-grained knowledge of the problem at hand in terms of material property, domain, and input to the solver and performance metrics, limiting the applicability of such modeling techniques for different constrained problems in engineering or even more challenging topology problems. The guidance requires the training of two additional models (a classification and a regression model) and is particularly useful with out-of-distribution configurations. However such guidance requires additional topologies, optimal and suboptimal, to train the regression model, assuming that we have access to the desired performance metric on the train set. Similarly for the classifier, where additional labeled data has to be gathered.

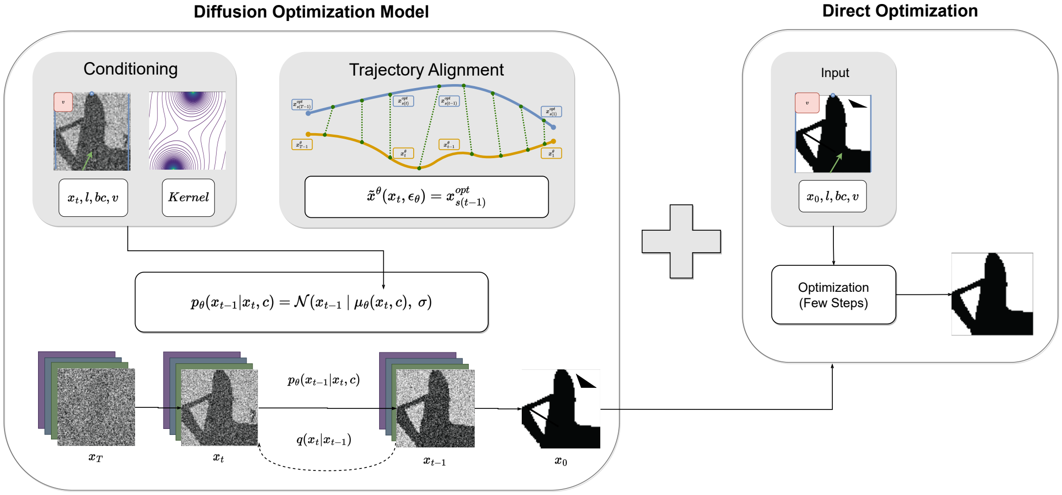

Figure 3: The DOM pipeline with conditioning and kernel relaxation (top left) and trajectory alignment (top right). The Diffusion Optimization Model generates design candidates, which are further refined using optimization tools. After the generation step (left side), we can improve the generated topology using a few steps of SIMP (5/10) to remove floating material and improve performance (right side).

3 Method

To tackle such limitations, we propose *Diffusion Optimization Models* (DOM), a conditional diffusion model with the goal of improving constrained design generation. One of our main goals is to improve inference time without loss in performance and constraint satisfaction. DOM is based on three main components: (i) Trajectory Alignment (Fig. 1 and Fig. 4) to ground sampling trajectory in the underlying physical process; (ii) Dense Kernel Relaxation (Fig. 5) to make preprocessing efficient; and (iii) Few-Steps Direct Optimization to improve out-of-distribution performance (Fig. 3 for an overview). See appendix A for algorithms with and without trajectory alignment.

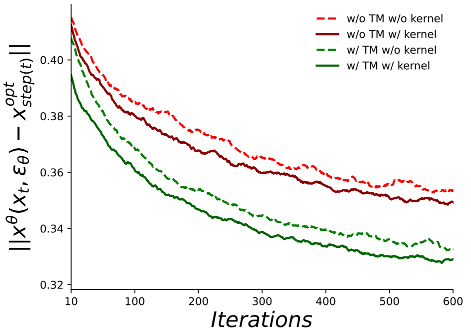

Figure 4: Distance between intermediate sampling steps in DOM and optimization steps with and without Trajectory Alignment. Given a random sampling step t and the corresponding optimization step $s(t) = \mod(t, n)$ where $n \in [2, 10]$. We compute the matching in clean space, using the approximate posterior q to obtain an estimate for $\mathbf{x}^{\theta}$ given $\mathbf{x}_t$ and the noise prediction ϵ_θ. Then we compute the distance $||\tilde{\mathbf{x}}^{\theta}(\mathbf{x}_t, \epsilon_\theta) - \mathbf{x}^{opt}_{s(t)}||_2$.

Trajectory Alignment (TA). Our goal is to align the sampling trajectory with the optimization trajectory, incorporating optimization in data-driven generative models by leveraging the hierarchical sampling structure of diffusion models. This aligns trajectories with physics-based information, as illustrated in

Fig. 1a. Unlike previous approaches, which use optimization as pre-processing or post-processing steps, trajectory alignment is performed during training and relies upon the marginalization property of diffusion models, i.e., $q(\mathbf{x}_t|\mathbf{x}_0) = \int q(\mathbf{x}_{1:t}|\mathbf{x}_0) d\mathbf{x}_{1:t-1}$, where $\mathbf{x}_t = \sqrt{\bar{\alpha}_t}\mathbf{x}_0 + (1 - \bar{\alpha}_t)\ \epsilon$, with $\epsilon \sim N(0, I)$. The trajectory alignment process can match in clean space (matching step 0), noisy space (matching step t), and performance space and leverage multi-fidelity mechanisms. At a high-level, TA is a regularization mechanism that injects an optimization-informed prior at each sampling step, forcing it to be close to the corresponding optimization step in terms of distance. This process provides a consistency mechanism [108, 104, 97] over trajectories and significantly reduces the computational cost of generating candidates without sacrificing accuracy.

Alignment Challenges. The alignment of sampling and optimization trajectories is challenging due to their differing lengths and structures. For example, the optimization trajectory starts with an image of all zeros, while the sampling path starts with random noise. Furthermore, Diffusion Models define a Stochastic Differential Equation (SDE, [106]) in the continuous limit, which represents a collection of trajectories, and the optimization trajectory cannot be directly represented within this set. To address these issues, trajectory alignment comprises two phases (see Figure 1b): a search phase and a matching phase. In the search phase, we aim to find the closest trajectory, among those that can be represented by the reverse process, to the optimization trajectory. This involves identifying a suitable representation over a trajectory that aligns with the optimization process. In the matching phase, we minimize the distance between points on the sampling and optimization trajectories to ensure proximity between points and enable alignment between trajectories.

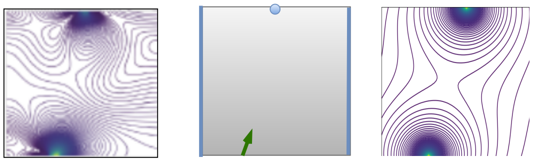

Figure 5: Comparison of iterative (left), sparse (center), and dense single-step (right) conditioning fields for a Constrained Diffusion Model. Unlike the expensive iterative FEA method, the physics-inspired fields offer a cost-effective, single-step approximation that's domain-agnostic and scalable.

Trajectory Search. We leverage the approximate posterior and marginalization properties of diffusion models to perform a trajectory search, using the generative model as a parametric guide to search for a suitable representation for alignment. Given an initial point $\mathbf{x}_0$, we obtain an approximate point $\mathbf{x}_t$ by sampling from the posterior distribution $q(\mathbf{x}_t|\mathbf{x}_0)$. We then predict $\epsilon_\theta(\mathbf{x}_t)$ with the model and use it to obtain $\tilde{\mathbf{x}}^\theta(\mathbf{x}_t, \epsilon_\theta(\mathbf{x}_t))$. In a DDPM, $\tilde{\mathbf{x}}^\theta$ is an approximation of $\mathbf{x}_0$ and is used as an intermediate step to sample $\mathbf{x}^\theta_{t-1}$ using the posterior functional form $q(\mathbf{x}^\theta_{t-1}|\mathbf{x}_t, \tilde{\mathbf{x}}^\theta)$. In DOM, we additionally leverage $\tilde{\mathbf{x}}^\theta$ to transport the sampling step towards a suitable representation for matching an intermediate optimization step $\mathbf{x}^{opt}_{step(t)}$ corresponding to t using some mapping. Trajectory alignment involves matching the optimization trajectory, which is an iterative exact solution for physics-based problems, with the sampling trajectory, which is the hierarchical sampling mechanism leveraged in Diffusion Models [43] and Hierarchical VAEs [100]. In practice, in DOM we sample $\mathbf{x}_t = \sqrt{\bar{\alpha}_t}\mathbf{x}_0 + (1 - \bar{\alpha}_t)\epsilon$ from $q(\mathbf{x}_t|\mathbf{x}_0)$ and run a forward step with the inverse process $\epsilon_\theta(\mathbf{x}_t, \mathbf{c})$ conditioning on the constraints $\mathbf{c}$ to obtain the matching representation $\tilde{\mathbf{x}}^\theta$ for step t:

$$\begin{aligned} \tilde{\mathbf{x}}^\theta &\sim q(\tilde{\mathbf{x}}^\theta|\tilde{\mu}^\theta(\mathbf{x}_t, \epsilon_\theta), \gamma) \\ \tilde{\mu}^\theta(\mathbf{x}_t, \epsilon_\theta) &= (\mathbf{x}_t - \sqrt{1 - \bar{\alpha}_t}\ \epsilon_\theta(\mathbf{x}_t, \mathbf{c}))/\sqrt{\bar{\alpha}_t}. \end{aligned} \tag{5}$$

Trajectory Matching. Then we match the distribution of matching representation $q(\tilde{\mathbf{x}}^\theta|\mathbf{x}_t, \epsilon_\theta)$ for sampling step t with the distribution of optimized representations $q(\mathbf{x}^{opt}_{s(t-1)}|\texttt{opt})$ at iteration s (corresponding to step $t - 1$) conditioning on the optimizer S. In general, given that the sampling steps will be different than the optimization steps, we use $s(t - 1) = \mod((t - 1), n_s)$ where n_s is the number of optimized iterations stored. [1] We then can train the model as a weighted sum of the conditional DDPM objective and the trajectory alignment regularization:

$$\mathcal{L}_{\texttt{DOM}} = \mathbb{E}_{q(\mathbf{x}_t|\mathbf{x}_0)}\Big[\mathbb{KL}[q(\mathbf{x}_{t-1}|\mathbf{x}_t, \mathbf{x}_0) \mid p_\theta(\mathbf{x}^\theta_{t-1}|\mathbf{x}_t, \mathbf{c})] + \mathbb{KL}[q(\tilde{\mathbf{x}}^\theta|\mathbf{x}_t, \epsilon_\theta) \mid q(\mathbf{x}_{s(t-1)}|\texttt{opt})]\Big]. \tag{6}$$

This mechanism effectively pushes the sampling trajectory at each step to match the optimization trajectory, distilling the optimizer during the reverse process training. In practice, following practice

[1] for example, if we store an optimized topology every 20 iterations for $S = 100$ steps, $n_s = 5$, and we sample a diffusion model for $T = 1000$, $s = 1$ for $(T : T - 200)$, and $s = 5$ for steps $(200 : 1)$.

in DDPM literature, the distribution variances are not learned from data. For the trajectory alignment distributions, we set the dispersion to the same values used in the model. By doing so we can rewrite the per-step negated lower-bound as a weighted sum of squared errors:

$$\mathcal{L}_{\texttt{DOM}} = \underbrace{\mathbb{E}_{q(\epsilon)}\left[w_t||\epsilon_\theta(\mathbf{x}_t(\mathbf{x}_0,\epsilon),\mathbf{c}) - \epsilon||_2^2\right]}_{L_{t-1,\epsilon}(\mathbf{x},\mathbf{c})} + \underbrace{\alpha_c||\tilde{\mathbf{x}}^\theta(\mathbf{x}_t,\epsilon_\theta) - \mathbf{x}^{opt}_{s(t-1)}||_2^2}_{\mathcal{L}^{\texttt{TA}}_{clean}} \tag{7}$$

where $\mathcal{L}^{\texttt{TA}}_{clean}$ is the trajectory alignment loss for step t, and $L_{t-1,\epsilon}(\mathbf{x},\mathbf{c})$ is a conditional DDPM loss for step t. This is the formulation employed for our model, where we optimize this loss for the mean values, freeze the mean representations, and optimize the variances in a separate step [68]. Alignment can also be performed in alternative ways. We can perform matching in noisy spaces, using the marginal posterior to obtain a noisy optimized representation for step $t-1$, $q(\mathbf{x}^{opt}_{t-1}|\mathbf{x}^{opt}_{s(0)})$ and then optimize $\mathcal{L}^{\texttt{TA}}_{noisy} = \alpha_n||\mathbf{x}^\theta_{t-1} - \mathbf{x}^{opt}_{t-1}||_2^2$. Finally, we can match in performance space: this approach leverages an auxiliary model f_ϕ similar to (consistency models) and performs trajectory alignment in functional space, $\mathcal{L}^{\texttt{TA}}_{perf} = \alpha_p||f_\phi(\mathbf{x}^\theta_{t-1}) - P_{s(t-1)}||_2$, where we match the performance for the generated intermediate design with the ground truth intermediate performance $P_{s(t-1)}$ for the optimized $\mathbf{x}^{opt}_{s(t-1)}$. We compare these and other variants in Table 6.

Dense Conditioning over Sparse Constraints. All models are subject to conditioning based on loads, boundary conditions, and volume fractions. In addition, TopoDiff and TopoDiff-GUIDED undergo conditioning based on force field and energy strain, while TopoDiff-FF and DOM are conditioned based on a dense kernel relaxation, inspired by Green's method [36, 34], which defines integral functions that are solutions to the time-invariant Poisson's Equation [33, 41]. More details are in Appendix B. The idea is to use the kernels as approximations to represent the effects of the boundary conditions and loads as smooth functions across the domain (Fig. 5). This approach avoids the need for computationally expensive and time-consuming Finite Element Analysis (FEA) to provide conditioning information. For a load or source l, a sink or boundary b and $r = ||\mathbf{x} - \mathbf{x}_l||_2 = \sqrt{(\mathbf{x}_i - \mathbf{x}^l_i)^2 + (\mathbf{x}_j - \mathbf{x}^l_j)^2}$, we have:

$$\begin{aligned} K_l(\mathbf{x},\mathbf{x}_l;\alpha) &= \textstyle\sum_{l=1}^{L}(1 - e^{-\alpha/||\mathbf{x}-\mathbf{x}_l||_2^2})\ \bar{p}(\mathbf{x}_l) \\ K_b(\mathbf{x},\mathbf{x}_b;\alpha) &= \textstyle\sum_{b=1}^{B} e^{-\alpha/||\mathbf{x}-\mathbf{x}_b||_2^2} / \max_{\mathbf{x}}\left(\textstyle\sum_{b=1}^{B} e^{-\alpha/||\mathbf{x}-\mathbf{x}_b||_2^2}\right). \end{aligned} \tag{8}$$

where $\bar{p}$ is the module of a generic force in 2D. Notice how, for $r \to 0$, $K_l(\mathbf{x},\mathbf{x}_l) \to p$, and $r \to \infty$, $K_l(\mathbf{x},\mathbf{x}_l) \to 0$. We notice how closer to the boundary the kernel is null, and farther from the boundary the kernel tends to 1. Note that the choice of α parameters in the kernels affects the smoothness and range of the kernel functions. Furthermore, these kernels are isotropic, meaning that they do not depend on the direction in which they are applied. Overall, the kernel relaxation method offers a computationally inexpensive way to condition generative models on boundary conditions and loads, making them more applicable in practical engineering and design contexts.

Few-Steps Direct Optimization. Finally, we leverage direct optimization to improve the data-driven candidate generated by DOM. In particular, by running a few steps of optimization (5/10) we can inject physics information into the generated design directly, greatly increasing not only performance but greatly increasing manufacturability. Given a sample from the model $\tilde{\mathbf{x}}_0 \sim p_\theta(\mathbf{x}_0|\mathbf{x}_1)p_\theta(\mathbf{x}_{1:T})$, we can post-process it and obtain $\mathbf{x}_0 = \texttt{opt}(\tilde{\mathbf{x}}^\theta_0, n)$ an improved design leveraging n steps of optimization, where $n \in [5, 10]$. In Fig. 3 we show a full pipeline for DOM.

4 Experiments

Our three main objectives are: (1) Improving inference efficiency, and reducing the sampling time for diffusion-based topology generation while still satisfying the design requirements with a minimum decrease in performance. (2) Minimizing reliance on force and strain fields as conditioning information, reducing the computation burden at inference time and the need for ad-hoc conditioning mechanisms for each problem. (3) Merging together learning-based and optimization-based methods, refining the topology generated using a conditional diffusion model, and improving the final solution in terms of manufacturability and performance.

Setup. We train all the models for 200k steps on 30k optimized topologies on a 64x64 domain. For each optimized topology, we have access to a small subset (5 steps) of intermediate optimization

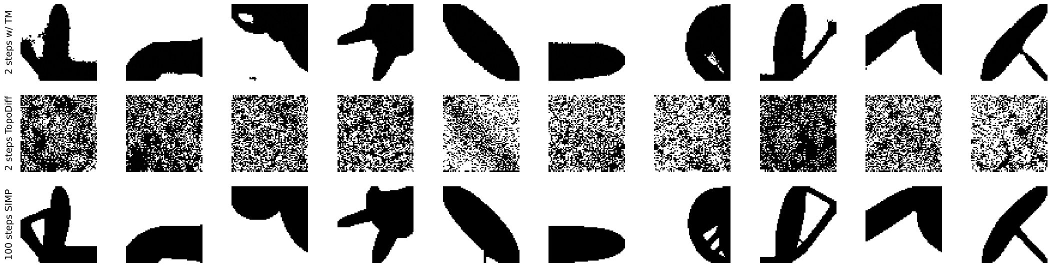

Figure 6: Few-Step sampling for Topology generation. Top row: Diffusion Optimization Model (DOM) with Trajectory Alignment. Middle row: TopoDiff-GUIDED. Bottom row: The optimization result. DOM produces high-quality designs in as few as two steps, greatly enhancing inference efficiency compared to previous models requiring 10-100 steps. Trajectory Alignment helps DOM generate near-optimal geometries swiftly, improving few-step sampling in conditional diffusion models for topology optimization. See appendix Fig. 11 for more examples.

steps. We set the hyperparameters, conditioning structure, and training routine as proposed in [62]. Appendix E for more details. For all the models (Table 9) we condition on volume fraction and loads. For TopoDiff, we condition additional stress and energy fields. For TopoDiff-FF [37], a variant of TopoDiff conditioning on a kernel relaxation, we condition on boundary conditions and kernels. TopoDiff-GUIDED leverages a compliance regressor and floating material classifier guidance. We use a reduced number of sampling steps for all the experiments.

Dataset. We use a dataset of optimized topologies gathered using SIMP as proposed in [66, 62]. Together with the topologies, the dataset contains information about optimal performance. For each topology, we have information about the loading condition, boundary condition, volume fraction, and optimal compliance. Additionally, for each constraint configuration, a pre-processing step computes the force and strain energy fields (see Fig. 5) when needed. Appendix D for more details on the dataset and visualizations.

Evaluation.

We evaluate the model using engineering and generative metrics. In particular, we consider metrics that evaluate how well our model fulfills: physical constraints using error wrt prescribed Volume Fraction (VFE); engineering constraints, as manufacturability as measured by Floating Material (FM); performance constraints, as measured by compliance error (CE) wrt the optimized SIMP solution; sampling time constraints (inference constraints) as measure by sampling time (inference and pre-processing). We consider two scenarios of increasing complexity: **(i)** In-distribution Constraints. The constraints in this test set are the same as those of the training set. When measuring performance on this set, we filter generated configurations with high compliance. **(ii)** Out-of-distribution Constraints. The constraints in this test set are different from those of the training set. When measuring performance on this set, we filter generated configurations with high compliance. The purpose of these tasks is to evaluate the generalization capability of the machine learning models in- and out-of-distribution. By testing the models on different test sets with varying levels of difficulty, we can assess how well the models can perform on new, unseen data. More importantly, we want to understand how important the role of the force field and energy strain is with unknown constraints.

Table 1: Comparative study of generative models in topology optimization considering factors like conditional input (COND), finite element method (FEM), and guidance (GUID). Unlike others, the DOM model operates without FEM preprocessing or GUIDANCE. More visualizations and optimization trajectories are in the Appendix.

	w/ COND	w/o FEM	w/o GUID
TopologyGAN [69]	✓	✗	✗
TopoDiff [62]	✓	✗	✓
TopoDiff-G [62]	✓	✗	✗
DOM (ours)	✓	✓	✓

In-Distribution Constraints. Table 3 reports the evaluation results in terms of constraints satisfaction and performance for the task of topology generation. In Table 2 we report metrics commonly employed to evaluate the quality of generative models in terms of fidelity (IS, sFID, P) and diversity (R). We see how such metrics are all close and it is challenging to gain any understanding just by relying on classic generative metrics when evaluating constrained design generation. These results justify the need for an evaluation that considers the performance and feasibility of the generated design.

In Table 3 DOM achieves high performance and is at least 50 % less computationally expensive at inference time, not requiring FEM preprocessing or additional guidance through surrogate models like TopologyGAN and TopoDiff. We also compare with Consistency Models [104], a Diffusion Model that tries to predict its input at each step. DOM can be seen as a generalization of such a method when a trajectory is available as a ground truth. Overall, DOM with Trajectory Alignment is competitive or better than the previous proposal in terms of performance on in-distribution constraints, providing strong evidence that TA is an effective mechanism to guide the sampling path toward regions of high performance.

Table 2: Generative metrics on in-distribution metrics. Precision denotes the fraction of generated topologies that are realistic, and recall measures the fraction of the training data manifold covered by the model.

	IS ↑	sFID ↓	P ↑	R ↑
cDDPM	3.41	40.30	0.73	0.85
TopoDiff	3.57	36.20	**0.80**	**0.86**
TopoDiff-G	3.63	**35.96**	0.79	**0.86**
DOM w/o TA	3.48	37.54	0.76	**0.86**
DOM w/ TA	**3.68**	36.73	0.77	0.85

Table 3: Evaluation of different model variants on in-distribution constraints. CE: Compliance Error. VFE: Volume Fraction Error. FM: Floating Material. We use 100 sampling steps for all diffusion models. We can see that DOM w/ TA is competitive with the SOTA on topology generation, being computationally 50 % less expensive at inference time compared to TopoDiff. Trajectory Alignment greatly improves performance without any additional inference cost. See the appendix Fig. 9 for confidence intervals.

	STEPS	CONSTRAINTS	AVG % CE ↓	MDN % CE ↓	% VFE ↓	% FM ↓	INFERENCE (s) ↓
TopologyGAN [69]	1	FIELD	48.51	2.06	11.87	46.78	3.37
Conditional DDPM [68]	100	RAW	60.79	3.15	1.72	8.72	**2.23**
Consistency Model [104]	100/1	KERNEL	10.30	2.20	1.64	8.72	2.35
TopoDiff-FF [37]	100	KERNEL	24.90	1.92	2.05	8.15	2.35
TopoDiff [62]	100	FIELD	5.46	0.80	**1.47**	**5.79**	5.54
TopoDiff-GUIDED [62]	100	FIELD	5.93	0.83	1.49	5.82	5.77
DOM w/o TA (ours)	100	KERNEL	13.61	1.79	1.86	7.44	2.35
DOM w/ TA (ours)	100	KERNEL	**4.44**	**0.74**	1.52	6.72	2.35

Table 4: Evaluating sampling topologies with few steps (2-10) for TopoDiff and DOM. G: Guided using regression and classifier guidance. AVG CE: average compliance error. MDN CE: median compliance error. VFE: volume fraction error. FM: floating material. INF: inference time. UNS: unsolvable configurations. LD: load disrespect. DOM largely outperforms TopoDiff in the few sampling step regimes, showing Trajectory Alignment's effectiveness as a grounding mechanism. DOM can generate reasonable topologies in just two sampling steps, where TopoDiff and DOM w/ TA fail completely, even presenting cases of load disrespect.

in-distro	STEPS	SIZE	AVG % CE ↓	MDN % CE ↓	% VFE ↓	% FM ↓	INF (s) ↓	% UNS ↓	% LD ↓
TopoDiff-G	2	239M	681.53	436.83	80.98	98.72	3.36	**2.00**	15.92
DOM (ours)	2	121M	**22.66**	**1.46**	**3.34**	**33.25**	**0.17** (- 94.94 %)	2.11	**0.00**
TopoDiff-G	5	239M	43.27	15.48	2.76	77.65	3.43	**1.44**	**0.00**
DOM (ours)	5	121M	**11.99**	**0.72**	**2.27**	**20.08**	**0.24** (- 93.00 %)	2.77	**0.00**
TopoDiff-G	10	239M	6.43	1.61	1.95	20.55	3.56	**0.00**	**0.00**
DOM (ours)	10	121M	**4.44**	**0.57**	**1.67**	**11.94**	**0.35** (- 90.17 %)	**0.00**	**0.00**
out-distro									
TopoDiff-G	2	239M	751.17	548.26	81.46	100.00	3.36	**1.90**	16.48
DOM (ours)	2	121M	**79.66**	**10.37**	**3.69**	**44.20**	**0.17** (- 94.94 %)	2.80	**0.00**
TopoDiff-G	5	239M	43.50	19.24	2.58	79.57	3.43	2.20	**0.00**
DOM (ours)	5	121M	**38.97**	**5.49**	**2.56**	**26.70**	**0.24** (- 93.00 %)	**1.40**	**0.00**
TopoDiff-G	10	239M	**10.78**	**2.55**	1.87	21.36	3.56	2.10	**0.00**
DOM (ours)	10	121M	32.19	3.69	**1.78**	**14.20**	**0.35** (- 90.17 %)	**0.40**	**0.00**

Generation with Few-Steps of Sampling. Table 4 compares two different algorithms, TopoDiff-GUIDED and DOM, in terms of their performance when using only a few steps for sampling. The table shows the results of the in and out-of-distribution comparison, with TopoDiff-G and DOM both having STEPS values of 2, 5, and 10, and SIZE of 239M and 121M. We can see that DOM outperforms by a large margin TopoDiff-G when tasked with generating a new topology given a few steps, corroborating our hypothesis that aligning the sampling and optimization trajectory is an effective mechanism to obtain efficient generative models that satisfy constraints. DOM outperforms

TopoDiff-GUIDED even being 50 % smaller, without leveraging an expensive FEM solver for conditioning but relying on cheap dense relaxations, making it 20/10 times faster at sampling, and greatly enhancing the quality of the generated designs, providing evidence that Trajectory Alignment is an effective mechanism to distill information from the optimization path. In Fig. 6, we provide qualitative results to show how DOM (top row) is able to generate reasonable topologies, resembling the fully optimized structure running SIMP for 100 steps (bottom row), with just two steps at inference time, where the same model without TA or a TopoDiff are not able to perform such task. Overall these results corroborate our thesis regarding the usefulness of trajectory alignment for high-quality constrained generation.

Merging Generative Models and Optimization for Out-of-Distribution Constraints. Table 5 shows the results of experiments on out-of-distribution constraints. In this scenario, employing FEM and guidance significantly enhances the performance of TopoDiff. Conditioning on the FEM output during inference can be seen as a form of test-time conditioning that can be adapted to the sample at hand. However, merging DOM and a few iterations of optimization is extremely effective in solving this problem, in particular in terms of improving volume fraction and floating material. Using the combination of DOM and SIMP is a way to impose the performance constraints in the model without the need for surrogate models or guidance.

Table 5: Out-of-Distribution Scenario Comparison: TopoDiff-G outperforms DOM due to its adaptive conditioning mechanism, which leverages expensive FEM-computed fields. However, DOM coupled with a few steps of direct optimization (5/10) greatly surpasses TopoDiff in performance and manufacturability. This underscores the effectiveness of integrating data-driven and optimization methods in constrained design creation.

	STEPS	MDN % CE $\downarrow$	% VFE $\downarrow$	% FM $\downarrow$
TopoDiff-FF	100	16.06	1.97	8.38
TopoDiff-G	100	1.82	1.80	6.21
DOM	100	3.47	1.59	8.02
DOM + SIMP	100+5	1.89	1.77	10.19
DOM + SIMP	100+10	**1.15**	**1.10**	**2.61**

Trajectory Alignment Ablation. The core contribution of DOM is trajectory alignment, a method to match sampling and optimization trajectories of arbitrary length and structure mapping intermediate steps to appropriate CLEAN (noise free or with reduced noise using the model and the marginalization properties of DDPM) representations. However, alignment can be performed in multiple ways, leveraging NOISY representation, matching performance (PERF), and using data at a higher resolution to impose consistency (MULTI). In Table 6 we perform an ablation study, considering DOM with and without kernel relaxation, and leveraging different kinds of trajectory matching. From the table, we see that using dense conditioning is extremely important for out-of-distribution performance, and that matching using CLEAN is the most effective method in and out-of-distribution. In Fig. 4 we report a visualization of the distance between sampling and optimization trajectory during training. From this plot, we can see how the kernel together with TA helps the model to find trajectories that are closer to the optimal one, again corroborating the need for dense conditioning and consistency regularization.

Table 6: Ablation study with and without kernel and trajectory alignment. We explore different ways to match the sampling and optimization trajectory and we measure the Median Compliance Error. TA: trajectory alignment. CM: Consistency Models [104].

	KERNEL	TA	MODE	IN-DISTRO	OUT-DISTRO
DOM	✗	✗	-	3.29	8.05
DOM	✗	✓	CLEAN	1.11	9.01
CM	✓	✗	-	2.20	5.25
DOM	✓	✗	-	1.80	5.62
DOM	✓	✓	MULTI	34.95	54.73
DOM	✓	✓	NOISY	2.08	6.23
DOM	✓	✓	PERF	2.41	6.82
DOM	✓	✓	CLEAN	**0.74**	**3.47**

Inference Time. With the previous experiments, we proved that a data-driven approach, biased towards the physical process, can distill the optimization process and sample a novel topology in a few steps. We then provide experiments for in and out-of-distribution and ablate our choice of kernel relaxation and trajectory alignment mechanism. However, the final goal of data-driven design is to learn a general tool for fast candidate generation. Here we compare inference time for different models and, more importantly, for low- (64) and high-resolution (256). Given the computational burden of training such models at high resolution, we train all the models for only 10k steps (around 5% of the full training), and then we use them for sampling. With this experiment, we want to emphasize how fast DOM can perform inference compared to a SOTA model. We choose to run all the generative models and optimized for 100 steps: this setting is not suited for DOM, because as we

Table 7: Inference time for different models at low and high resolution. For all the diffusion models we sample 100 steps and for SIMP we iterate for 100 steps. *We report optimization time for a full comparison, but it is important to emphasize that SIMP runs on CPU and the DDPM-based models on GPU. $\Delta T_{inference} = (T_{model} - T_{topodiff})/T_{topodiff}$.

	RES	SIZE	PREPROCESS	POSTPROCESS	SAMPLING	INFERENCE	$\Delta T_{inference}$
TopoDiff	64	121M	3.31	0.00	2.23	5.54	+ 0.00 %
TopoDiff-GUIDED	64	239M	3.31	0.00	2.46	5.77	+ 4.15 %
DOM (ours)	64	121M	0.12	0.00	2.23	**2.35**	- 57.58 %
SIMP	64	-	0.00	18.12	0.00	18.12	+ 227.07 %*
TopoDiff	256	553M	31.84	0.00	7.78	38.62	+ 0.00 %
TopoDiff-GUIDED	256	1092M	31.84	0.00	8.46	40.30	+ 4.35 %
DOM (ours)	256	553M	0.31	0.00	7.78	**8.09**	- 79.05 %
SIMP	256	-	0.00	316.02	0.00	316.02	+ 718.28 %*

have seen the model excels in the few-step sampling task. Table 7 presents a comparison of various models based on different factors such as resolution (RES), size, preprocess time, postprocess time, sampling, and inference time.

5 Related Work

Topology Optimization. Engineering design is the process of creating solutions to technical problems under engineering requirements [22, 91, 23]. Often, the goal is to create highly performative designs given the required constraints. Topology Optimization (TO [14]) is a branch of engineering design and is a critical component of the design process in many industries, including aerospace, automotive, manufacturing, and software development. From the inception of the homogenization method for TO, a number of different approaches have been proposed, including density-based [13, 86, 64], level-set [3, 111], derivative-based [99], evolutionary [115], and others [19]. The density-based methods are widely used and use a nodal-based representation where the level-set leverages shape derivative to obtain the optimal topology. To improve the final design, filtering mechanisms have been proposed [117, 39, 94]. Hybrid methods are also widely used. Topology Optimization has evolved as a more and more intensive computational discipline, with the availability of efficient open-source implementations [92, 93, 46, 59, 4]. See [59] for more on this topic. See [95, 96] for a comprehensive review of the Topology Optimization field.

Generative Models for Topology Optimization. Following the success of Deep Learning (DL) in vision, a surging interest arose recently for transferring these methods to the engineering field. In particular, DL methods have been employed for direct-design [1, 5, 11, 60, 110], accelating the optimization process [7, 49, 52, 107, 118], improving the shape optimization post-processing [42, 119], super-resolution [32, 65, 120], sensitivity analysis [6, 75, 10, 89], 3d topologies [54, 87, 11], and more [26, 24, 25, 29]. Among these methods, Generative Models are especially appealing to improve design diversity in engineering design [2, 72, 70, 71]. In TO, the work of [47, 82, 83, 55, 109] focus on increasing diversity leveraging data-driven approaches. Additionally, Generative Models have been used for Topology Optimization problems conditioning on constraints (loads, boundary conditions, volume fraction for the structural case), directly generating topologies [81, 90, 40] training dataset of optimized topologies, leveraging superresolution methods to improve fidelity [121, 58], using filtering and iterative design approaches [74, 73, 17, 35] to improve quality and diversity. Methods for 3D topologies have also been proposed [12, 55]. Recently, GAN [69] and DDPM-based [62] approaches, conditioning on constraints and physical information, have had success in modeling the TO problem. For a comprehensive review and critique of the field, see [113].

Conditional Diffusion Models. Methods to condition DDPM have been proposed, conditioning at sampling time [28], learning a class-conditional score [106], explicitly conditioning on class information [68], features [38, 9], and physical properties [116, 45]. Recently, TopoDiff [62] has shown that conditional diffusion models with guidance [31] are effective for generating topologies that fulfill the constraints and have high manufacturability and high performance. TopoDiff relies on physics information and surrogate models to guide the sampling of novel topologies with good performance. Alternatives to speed up sampling in TopoDiff have been recently proposed [37], trading performance for fast candidate generation. Improving efficiency and sampling speed for diffusion models is an active research topic, both reducing the number of sampling steps [68, 103, 102, 8], improving the ODE solver [48, 112, 57], leveraging distillation [88, 63], and exploiting autoencoders for dimensionality reduction [85, 77, 76]. Reducing the number of sampling steps can also be achieved by improving the property of the hierarchical latent space, exploiting a form of consistency regularization [108, 97, 122] during training. Consistency Models [104] proposes reconstructing its input from any step in the diffusion chain, effectively forcing the model to reduce the sampling steps needed for high-quality sampling. We similarly want to improve the latent space properties but leverage trajectory alignment with a physical process. Recently, energy-constrained diffusion models [114] have been proposed to regularize graph learning a learn expressive representations for structured data.

6 Conclusion

We presented Diffusion Optimization Models, a generative framework to align the sampling trajectory with the underlying physical process, and learn an efficient and expressive generative model for constrained engineering design. Our work opens new avenues for improving generative design in engineering and related fields. However, our method is limited by the capacity to store and retrieve intermediate optimization steps, and, without a few steps of optimization, it underperforms out-of-distribution compared to FEM-conditional and guided methods.

Acknowledgement

We would like to thank Noah Joseph Bagazinski, Kristen Marie Edwards, Amin Heyrani Nobari, Cyril Picard, Lyle Regenwetter and Binyang Song for insightful comments and useful discussions.

References

[1] D. W. Abueidda, S. Koric, and N. A. Sobh. Topology optimization of 2D structures with nonlinearities using deep learning. *Computers & Structures*, 237:106283, 9 2020.

[2] F. Ahmed, M. Fuge, and L. D. Gorbunov. Discovering diverse, high quality design ideas from a large corpus. In *International Design Engineering Technical Conferences and Computers and Information in Engineering Conference*, volume 50190, page V007T06A008. American Society of Mechanical Engineers, 2016.

[3] G. Allaire, F. Jouve, and A.-M. Toader. A level-set method for shape optimization. *Comptes Rendus Mathematique*, 334(12):1125–1130, 2002.

[4] E. Andreassen, A. Clausen, M. Schevenels, B. S. Lazarov, and O. Sigmund. Efficient topology optimization in MATLAB using 88 lines of code. *Structural and Multidisciplinary Optimization*, 43(1):1–16, 1 2011.

[5] G. C. Ates and R. M. Gorguluarslan. Two-stage convolutional encoder-decoder network to improve the performance and reliability of deep learning models for topology optimization. *Structural and Multidisciplinary Optimization*, 63(4):1927–1950, 4 2021.

[6] N. Aulig and M. Olhofer. Evolutionary generation of neural network update signals for the topology optimization of structures. In *Proceedings of the 15th annual conference companion on Genetic and evolutionary computation*, pages 213–214, New York, NY, USA, 7 2013. ACM.

[7] S. Banga, H. Gehani, S. Bhilare, S. Patel, and L. Kara. 3D Topology Optimization using Convolutional Neural Networks. *Preprint*, 8 2018.

[8] F. Bao, C. Li, J. Zhu, and B. Zhang. Analytic-dpm: an analytic estimate of the optimal reverse variance in diffusion probabilistic models. *arXiv preprint arXiv:2201.06503*, 2022.

[9] D. Baranchuk, I. Rubachev, A. Voynov, V. Khrulkov, and A. Babenko. Label-efficient semantic segmentation with diffusion models. *arXiv preprint arXiv:2112.03126*, 2021.

[10] S. Barmada, N. Fontana, A. Formisano, D. Thomopulos, and M. Tucci. A Deep Learning Surrogate Model for Topology Optimization. *IEEE Transactions on Magnetics*, 57(6):1–4, 6 2021.

[11] M. M. Behzadi and H. T. Ilieş. Real-time topology optimization in 3d via deep transfer learning. *Computer-Aided Design*, 135:103014, 2021.

[12] M. M. Behzadi and H. T. Ilieş. Real-Time Topology Optimization in 3D via Deep Transfer Learning. *Computer-Aided Design*, 135:103014, 6 2021.

[13] M. P. Bendsøe. Optimal shape design as a material distribution problem. *Structural optimization*, 1:193–202, 1989.

[14] M. P. Bendsøe and N. Kikuchi. Generating optimal topologies in structural design using a homogenization method. *Computer methods in applied mechanics and engineering*, 71(2):197–224, 1988.

[15] M. P. Bendsøe and N. Kikuchi. Generating optimal topologies in structural design using a homogenization method. *Computer Methods in Applied Mechanics and Engineering*, 71(2):197–224, 1988.

[16] L. Bers, F. John, and M. Schechter. *Partial differential equations*. American Mathematical Soc., 1964.

[17] D. Berthelot, T. Schumm, and L. Metz. Began: Boundary equilibrium generative adversarial networks. *arXiv preprint arXiv:1703.10717*, 2017.

[18] A. Blattmann, R. Rombach, K. Oktay, and B. Ommer. Retrieval-augmented diffusion models. *arXiv preprint arXiv:2204.11824*, 2022.

[19] B. Bourdin and A. Chambolle. Design-dependent loads in topology optimization. *ESAIM: Control, Optimisation and Calculus of Variations*, 9:19–48, 2003.

[20] A. Brock, J. Donahue, and K. Simonyan. Large scale gan training for high fidelity natural image synthesis. *arXiv preprint arXiv:1809.11096*, 2018.

[21] T. B. Brown, B. Mann, N. Ryder, M. Subbiah, J. Kaplan, P. Dhariwal, A. Neelakantan, P. Shyam, G. Sastry, A. Askell, et al. Language models are few-shot learners. *arXiv preprint arXiv:2005.14165*, 2020.

[22] R. G. Budynas, J. K. Nisbett, et al. *Shigley's mechanical engineering design*, volume 9. McGraw-Hill New York, 2011.

[23] D. M. Buede and W. D. Miller. The engineering design of systems: models and methods. 2016.

[24] A. Chandrasekhar, S. Sridhara, and K. Suresh. Gm-tounn: Graded multiscale topology optimization using neural networks. *arXiv preprint arXiv:2204.06682*, 2022.

[25] A. Chandrasekhar and K. Suresh. Multi-Material Topology Optimization Using Neural Networks. *Computer-Aided Design*, 136:103017, 7 2021.

[26] H. Chen, K. S. Whitefoot, and L. B. Kara. Concurrent build direction, part segmentation, and topology optimization for additive manufacturing using neural networks. In *International Design Engineering Technical Conferences and Computers and Information in Engineering Conference*, volume 86229, page V03AT03A029. American Society of Mechanical Engineers, 2022.

[27] R. Child. Very deep vaes generalize autoregressive models and can outperform them on images. *arXiv preprint arXiv:2011.10650*, 2020.

[28] J. Choi, S. Kim, Y. Jeong, Y. Gwon, and S. Yoon. Ilvr: Conditioning method for denoising diffusion probabilistic models. *arXiv preprint arXiv:2108.02938*, 2021.

[29] H. Deng and A. C. To. A Parametric Level Set Method for Topology Optimization based on Deep Neural Network (DNN). *Preprint*, 1 2021.

[30] J. Devlin, M.-W. Chang, K. Lee, and K. Toutanova. Bert: Pre-training of deep bidirectional transformers for language understanding. *arXiv preprint arXiv:1810.04805*, 2018.

[31] P. Dhariwal and A. Nichol. Diffusion models beat gans on image synthesis. *Advances in Neural Information Processing Systems*, 34, 2021.

[32] M. O. Elingaard, N. Aage, J. A. Bærentzen, and O. Sigmund. De-homogenization using convolutional neural networks. *Computer Methods in Applied Mechanics and Engineering*, 388:114197, 1 2022.

[33] L. C. Evans. *Partial differential equations*, volume 19. American Mathematical Society, 2022.

[34] A. Friedman. *Partial differential equations of parabolic type*. Courier Dover Publications, 2008.

[35] K. Fujita, K. Minowa, Y. Nomaguchi, S. Yamasaki, and K. Yaji. Design concept generation with variational deep embedding over comprehensive optimization. In *International Design Engineering Technical Conferences and Computers and Information in Engineering Conference, IDETC-21*, Virtual, Online, Aug 2021. ASME.

[36] P. Garabedian. Partial differential equations with more than two independent variables in the complex domain. *Journal of Mathematics and Mechanics*, pages 241–271, 1960.

[37] G. Giannone and F. Ahmed. Diffusing the optimal topology: A generative optimization approach. *arXiv preprint arXiv:2303.09760*, 2023.

[38] G. Giannone, D. Nielsen, and O. Winther. Few-shot diffusion models. *arXiv preprint arXiv:2205.15463*, 2022.

[39] J. K. Guest, J. H. Prévost, and T. Belytschko. Achieving minimum length scale in topology optimization using nodal design variables and projection functions. *International journal for numerical methods in engineering*, 61(2):238–254, 2004.

[40] T. Guo, D. J. Lohan, R. Cang, M. Y. Ren, and J. T. Allison. An indirect design representation for topology optimization using variational autoencoder and style transfer. In *2018 AIAA/ASCE/AHS/ASC Structures, Structural Dynamics, and Materials Conference*, page 0804, 2018.

[41] J. K. Hale and S. M. V. Lunel. *Introduction to functional differential equations*, volume 99. Springer Science & Business Media, 2013.

[42] N. Hertlein, P. R. Buskohl, A. Gillman, K. Vemaganti, and S. Anand. Generative adversarial network for early-stage design flexibility in topology optimization for additive manufacturing. *Journal of Manufacturing Systems*, 59:675–685, 4 2021.

[43] J. Ho, A. Jain, and P. Abbeel. Denoising diffusion probabilistic models. In H. Larochelle, M. Ranzato, R. Hadsell, M. Balcan, and H. Lin, editors, *Advances in Neural Information Processing Systems*, volume 33, pages 6840–6851. Curran Associates, Inc., 2020.

[44] J. Ho, A. Jain, and P. Abbeel. Denoising diffusion probabilistic models. In *Advances in Neural Information Processing Systems 33*, 2020.

[45] E. Hoogeboom, V. G. Satorras, C. Vignac, and M. Welling. Equivariant diffusion for molecule generation in 3d. *arXiv preprint arXiv:2203.17003*, 2022.

[46] W. Hunter et al. Topy-topology optimization with python, 2017.

[47] J. Jiang, M. Chen, and J. A. Fan. Deep neural networks for the evaluation and design of photonic devices. *Nature Reviews Materials*, 6(8):679–700, 8 2021.

[48] A. Jolicoeur-Martineau, K. Li, R. Piché-Taillefer, T. Kachman, and I. Mitliagkas. Gotta go fast when generating data with score-based models. *arXiv preprint arXiv:2105.14080*, 2021.

[49] Y. Joo, Y. Yu, and I. G. Jang. Unit Module-Based Convergence Acceleration for Topology Optimization Using the Spatiotemporal Deep Neural Network. *IEEE Access*, 9:149766–149779, 2021.

[50] M. I. Jordan, Z. Ghahramani, T. S. Jaakkola, and L. K. Saul. An introduction to variational methods for graphical models. *Machine learning*, 37(2):183–233, 1999.

[51] J. Jumper, R. Evans, A. Pritzel, T. Green, M. Figurnov, O. Ronneberger, K. Tunyasuvunakool, R. Bates, A. Žídek, A. Potapenko, et al. Highly accurate protein structure prediction with alphafold. *Nature*, 596(7873):583–589, 2021.

[52] N. A. Kallioras, G. Kazakis, and N. D. Lagaros. Accelerated topology optimization by means of deep learning. *Structural and Multidisciplinary Optimization*, 62(3):1185–1212, 9 2020.

[53] M. V. Keldysh. On the characteristic values and characteristic functions of certain classes of non-self-adjoint equations. In *Dokl. Akad. Nauk SSSR*, volume 77, pages 11–14, 1951.

[54] S. Kench and S. J. Cooper. Generating three-dimensional structures from a two-dimensional slice with generative adversarial network-based dimensionality expansion. *Nature Machine Intelligence*, 3(4):299–305, 2021.

[55] V. Keshavarzzadeh, M. Alirezaei, T. Tasdizen, and R. M. Kirby. Image-based multiresolution topology optimization using deep disjunctive normal shape model. *Computer-Aided Design*, 130:102947, 2021.

[56] D. P. Kingma and M. Welling. Auto-encoding variational bayes. *arXiv preprint arXiv:1312.6114*, 2013.

[57] Z. Kong and W. Ping. On fast sampling of diffusion probabilistic models. *arXiv preprint arXiv:2106.00132*, 2021.

[58] B. Li, C. Huang, X. Li, S. Zheng, and J. Hong. Non-iterative structural topology optimization using deep learning. *Computer-Aided Design*, 115:172–180, 2019.

[59] K. Liu and A. Tovar. An efficient 3d topology optimization code written in matlab. *Structural and Multidisciplinary Optimization*, 50:1175–1196, 2014.

[60] F. Ma and Z. Zeng. High-risk prediction localization: evaluating the reliability of black box models for topology optimization. *Structural and Multidisciplinary Optimization*, 62(6):3053–3069, 12 2020.

[61] M. Manica, J. Cadow, D. Christofidellis, A. Dave, J. Born, D. Clarke, Y. G. N. Teukam, S. C. Hoffman, M. Buchan, V. Chenthamarakshan, et al. Gt4sd: Generative toolkit for scientific discovery. *arXiv preprint arXiv:2207.03928*, 2022.

[62] F. Mazé and F. Ahmed. Diffusion models beat gans on topology optimization. In *Proceedings of the AAAI Conference on Artificial Intelligence (AAAI)*, Washington, DC, 2023.

[63] C. Meng, R. Gao, D. P. Kingma, S. Ermon, J. Ho, and T. Salimans. On distillation of guided diffusion models. *arXiv preprint arXiv:2210.03142*, 2022.

[64] H. Mlejnek. Some aspects of the genesis of structures. *Structural optimization*, 5:64–69, 1992.

[65] N. Napier, S.-A. Sriraman, H. T. Tran, and K. A. James. An Artificial Neural Network Approach for Generating High-Resolution Designs From Low-Resolution Input in Topology Optimization. *Journal of Mechanical Design*, 142(1), 1 2020.

[66] A. Nichol and P. Dhariwal. Improved denoising diffusion probabilistic models. *CoRR*, 2021.

[67] A. Nichol, P. Dhariwal, A. Ramesh, P. Shyam, P. Mishkin, B. McGrew, I. Sutskever, and M. Chen. Glide: Towards photorealistic image generation and editing with text-guided diffusion models. *arXiv preprint arXiv:2112.10741*, 2021.

[68] A. Q. Nichol and P. Dhariwal. Improved denoising diffusion probabilistic models. In *International Conference on Machine Learning*, pages 8162–8171. PMLR, 2021.

[69] Z. Nie, T. Lin, H. Jiang, and L. B. Kara. Topologygan: Topology optimization using generative adversarial networks based on physical fields over the initial domain. *Journal of Mechanical Design*, 143(3), 2021.

[70] A. H. Nobari, W. Chen, and F. Ahmed. Pcdgan: A continuous conditional diverse generative adversarial network for inverse design. *arXiv preprint arXiv:2106.03620*, 2021.

[71] A. H. Nobari, W. Chen, and F. Ahmed. Range-constrained generative adversarial network: Design synthesis under constraints using conditional generative adversarial networks. *Journal of Mechanical Design*, 144(2), 2022.

[72] A. H. Nobari, M. F. Rashad, and F. Ahmed. Creativegan: Editing generative adversarial networks for creative design synthesis. In *International Design Engineering Technical Conferences and Computers and Information in Engineering Conference, IDETC-21*, Virtual, Online, Aug 2021. ASME.

[73] S. Oh, Y. Jung, S. Kim, I. Lee, and N. Kang. Deep Generative Design: Integration of Topology Optimization and Generative Models. *Journal of Mechanical Design*, 141(11), 09 2019. 111405.

[74] S. Oh, Y. Jung, I. Lee, and N. Kang. Design automation by integrating generative adversarial networks and topology optimization. In *International Design Engineering Technical Conferences and Computers and Information in Engineering Conference*, volume 51753, page V02AT03A008. American Society of Mechanical Engineers, 2018.

[75] M. Olhofer, E. Oñate, J. Oliver, A. Huerta, and N. Aulig. TOPOLOGY OPTIMIZATION BY PREDICTING SENSITIVITIES BASED ON LOCAL STATE FEATURES. Technical report, 2014.

[76] K. Pandey, A. Mukherjee, P. Rai, and A. Kumar. Diffusevae: Efficient, controllable and high-fidelity generation from low-dimensional latents. *arXiv preprint arXiv:2201.00308*, 2022.

[77] K. Preechakul, N. Chatthee, S. Wizadwongsa, and S. Suwajanakorn. Diffusion autoencoders: Toward a meaningful and decodable representation. *arXiv preprint arXiv:2111.15640*, 2021.

[78] C. Raffel, N. Shazeer, A. Roberts, K. Lee, S. Narang, M. Matena, Y. Zhou, W. Li, and P. J. Liu. Exploring the limits of transfer learning with a unified text-to-text transformer. *The Journal of Machine Learning Research*, 21(1):5485–5551, 2020.

[79] A. Ramesh, P. Dhariwal, A. Nichol, C. Chu, and M. Chen. Hierarchical text-conditional image generation with clip latents. *arXiv preprint arXiv:2204.06125*, 2022.

[80] A. Ramesh, M. Pavlov, G. Goh, S. Gray, C. Voss, A. Radford, M. Chen, and I. Sutskever. Zero-shot text-to-image generation. In *International Conference on Machine Learning*, pages 8821–8831. PMLR, 2021.

[81] S. Rawat and M. H. Shen. Application of adversarial networks for 3d structural topology optimization. Technical report, SAE Technical Paper, 2019.

[82] S. Rawat and M. H. H. Shen. A novel topology design approach using an integrated deep learning network architecture. *Preprint*, 8 2018.

[83] S. Rawat and M. H. H. Shen. A Novel Topology Optimization Approach using Conditional Deep Learning. *Preprint*, 1 2019.

[84] L. Regenwetter, A. H. Nobari, and F. Ahmed. Deep generative models in engineering design: A review. *Journal of Mechanical Design*, 144(7):071704, 2022.

[85] R. Rombach, A. Blattmann, D. Lorenz, P. Esser, and B. Ommer. High-resolution image synthesis with latent diffusion models. *arXiv preprint arXiv:2112.10752*, 2021.

[86] G. I. Rozvany, M. Zhou, and T. Birker. Generalized shape optimization without homogenization. *Structural optimization*, 4:250–252, 1992.

[87] G. Sabiston and I. Y. Kim. 3d topology optimization for cost and time minimization in additive manufacturing. *Structural and Multidisciplinary Optimization*, 61(2):731–748, 2020.

[88] T. Salimans and J. Ho. Progressive distillation for fast sampling of diffusion models. *arXiv preprint arXiv:2202.00512*, 2022.

[89] H. Sasaki and H. Igarashi. Topology Optimization Accelerated by Deep Learning. *IEEE Transactions on Magnetics*, 55(6):1–5, 6 2019.

[90] C. Sharpe and C. C. Seepersad. Topology design with conditional generative adversarial networks. In *International Design Engineering Technical Conferences and Computers and Information in Engineering Conference*, volume 59186, page V02AT03A062. American Society of Mechanical Engineers, 2019.

[91] J. E. Shigley, L. D. Mitchell, and H. Saunders. Mechanical engineering design. 1985.

[92] O. Sigmund. A 99 line topology optimization code written in matlab. *Struct. Multidiscip. Optim.*, 21(2):120–127, apr 2001.

[93] O. Sigmund. A 99 line topology optimization code written in matlab. *Structural and multidisciplinary optimization*, 21:120–127, 2001.

[94] O. Sigmund. Morphology-based black and white filters for topology optimization. *Structural and Multidisciplinary Optimization*, 33:401–424, 2007.

[95] O. Sigmund and K. Maute. Topology optimization approaches: A comparative review. *Structural and Multidisciplinary Optimization*, 48(6):1031–1055, 2013.

[96] O. Sigmund and K. Maute. Topology optimization approaches: A comparative review. *Structural and Multidisciplinary Optimization*, 48(6):1031–1055, 2013.

[97] S. Sinha and A. B. Dieng. Consistency regularization for variational auto-encoders. *Advances in Neural Information Processing Systems*, 34:12943–12954, 2021.

[98] J. Sohl-Dickstein, E. Weiss, N. Maheswaranathan, and S. Ganguli. Deep unsupervised learning using nonequilibrium thermodynamics. In F. Bach and D. Blei, editors, *Proceedings of the 32nd International Conference on Machine Learning*, volume 37 of *Proceedings of Machine Learning Research*, pages 2256–2265, Lille, France, 07–09 Jul 2015. PMLR.

[99] J. Sokolowski and A. Zochowski. On the topological derivative in shape optimization. *SIAM journal on control and optimization*, 37(4):1251–1272, 1999.

[100] C. K. Sønderby, T. Raiko, L. Maaløe, S. K. Sønderby, and O. Winther. Ladder variational autoencoders. In *Advances in neural information processing systems*, pages 3738–3746, 2016.

[101] B. Song, R. Zhou, and F. Ahmed. Multi-modal machine learning in engineering design: A review and future directions. *arXiv preprint arXiv:2302.10909*, 2023.

[102] J. Song, C. Meng, and S. Ermon. Denoising diffusion implicit models. *arXiv preprint arXiv:2010.02502*, 2020.

[103] J. Song, C. Meng, and S. Ermon. Denoising diffusion implicit models. In *International Conference on Learning Representations*, 2021.

[104] Y. Song, P. Dhariwal, M. Chen, and I. Sutskever. Consistency models. *arXiv preprint arXiv:2303.01469*, 2023.

[105] Y. Song and S. Ermon. Generative modeling by estimating gradients of the data distribution. In *Advances in Neural Information Processing Systems 32*, 2019.

[106] Y. Song, J. Sohl-Dickstein, D. P. Kingma, A. Kumar, S. Ermon, and B. Poole. Score-based generative modeling through stochastic differential equations. *arXiv preprint arXiv:2011.13456*, 2020.

[107] I. Sosnovik and I. Oseledets. Neural networks for topology optimization. *Preprint*, 9 2017.

[108] A. Srivastava, L. Valkov, C. Russell, M. U. Gutmann, and C. Sutton. Veegan: Reducing mode collapse in gans using implicit variational learning. *Advances in neural information processing systems*, 30, 2017.

[109] H. Sun and L. Ma. Generative Design by Using Exploration Approaches of Reinforcement Learning in Density-Based Structural Topology Optimization. *Designs*, 4(2):10, 5 2020.

[110] E. Ulu, R. Zhang, and L. B. Kara. A data-driven investigation and estimation of optimal topologies under variable loading configurations. *Computer Methods in Biomechanics and Biomedical Engineering: Imaging & Visualization*, 4(2):61–72, 3 2016.

[111] M. Y. Wang, X. Wang, and D. Guo. A level set method for structural topology optimization. *Computer Methods in Applied Mechanics and Engineering*, 192(1-2):227–246, 1 2003.

[112] D. Watson, J. Ho, M. Norouzi, and W. Chan. Learning to efficiently sample from diffusion probabilistic models. *arXiv preprint arXiv:2106.03802*, 2021.

[113] R. V. Woldseth, N. Aage, J. A. Bærentzen, and O. Sigmund. On the use of artificial neural networks in topology optimisation. *Structural and Multidisciplinary Optimization*, 65(10):294, 2022.

[114] Q. Wu, C. Yang, W. Zhao, Y. He, D. Wipf, and J. Yan. Difformer: Scalable (graph) transformers induced by energy constrained diffusion. *arXiv preprint arXiv:2301.09474*, 2023.

[115] Y. M. Xie, G. P. Steven, Y. Xie, and G. Steven. *Basic evolutionary structural optimization*. Springer, 1997.

[116] M. Xu, L. Yu, Y. Song, C. Shi, S. Ermon, and J. Tang. Geodiff: A geometric diffusion model for molecular conformation generation. *arXiv preprint arXiv:2203.02923*, 2022.

[117] S. Xu, Y. Cai, and G. Cheng. Volume preserving nonlinear density filter based on heaviside functions. *Structural and Multidisciplinary Optimization*, 41:495–505, 2010.

[118] L. Xue, J. Liu, G. Wen, and H. Wang. Efficient, high-resolution topology optimization method based on convolutional neural networks. *Frontiers of Mechanical Engineering*, 16(1):80–96, 3 2021.

[119] A. Yildiz, N. Öztürk, N. Kaya, and F. Öztürk. Integrated optimal topology design and shape optimization using neural networks. *Structural and Multidisciplinary Optimization*, 25(4):251–260, 10 2003.

[120] S. Yoo, S. Lee, S. Kim, K. H. Hwang, J. H. Park, and N. Kang. Integrating deep learning into CAD/CAE system: generative design and evaluation of 3D conceptual wheel. *Structural and Multidisciplinary Optimization*, 64(4):2725–2747, 10 2021.

[121] Y. Yu, T. Hur, J. Jung, and I. G. Jang. Deep learning for determining a near-optimal topological design without any iteration. *Structural and Multidisciplinary Optimization*, 59(3):787–799, 2019.

[122] J.-Y. Zhu, T. Park, P. Isola, and A. A. Efros. Unpaired image-to-image translation using cycle-consistent adversarial networks. In *Proceedings of the IEEE international conference on computer vision*, pages 2223–2232, 2017.

A Algorithms

Algorithm 1 `DOM with Trajectory Alignment`

```
Require: Optimized Topologies $\mathbf{X}_0$
Require: Constraints $C = (BC, L, VF)$
Require: Intermediate Optimization Steps $\mathbf{X}^{opt}$
  while Training do
      Sample batch $(\mathbf{x}_0, c, \mathbf{x}^{opt})$
      Compute Dense Relaxation $k = K(bc, l)$
      Compute Conditioning $\mathbf{c} = (k, c)$
      Sample $t$, $\epsilon$, $\mathbf{x}^{opt}_{s(t)}$
      Compute $\mathbf{x}_t \sim q(\mathbf{x}_t|\mathbf{x}_0)$
      Forward Model $\epsilon_\theta(\mathbf{x}_t, \mathbf{c})$
      Compute Loss $L_{t-1}(\mathbf{x}, \mathbf{c}) = ||\epsilon_\theta(\mathbf{x}_t, \mathbf{c}) - \epsilon||_2^2$
      Trajectory Search $\tilde{\mathbf{x}}^\theta(\mathbf{x}_t, \epsilon_\theta) = (\mathbf{x}_t - \sqrt{1 - \bar{\alpha}_t}\ \epsilon_\theta(\mathbf{x}_t, \mathbf{c}))/\sqrt{\bar{\alpha}_t}$
      Trajectory Matching $\mathcal{L}_{\mathtt{TA}} = ||\tilde{\mathbf{x}}^\theta(\mathbf{x}_t, \epsilon_\theta) - \mathbf{x}^{opt}_{s(t)}||_2^2$
      Compute Loss $\mathcal{L}_{\mathtt{DOM}}(\theta) = L_{t-1}(\mathbf{x}, \mathbf{c}) + \mathcal{L}_{\mathtt{TA}}$
      Backpropagate $\theta \leftarrow \nabla_\theta \mathcal{L}_{\mathtt{DOM}}(\theta)$
  end while
```

Algorithm 2 `DOM without Trajectory Alignment`

```
Require: Optimized Topologies $\mathbf{X}_0$
Require: Constraints $C = (BC, L, VF)$
  while Training do
      Sample batch $(\mathbf{x}_0, c)$
      Compute Dense Relaxation $k = K(bc, l)$
      Compute Conditioning $\mathbf{c} = (k, c)$
      Sample $t$, $\epsilon$
      Compute $\mathbf{x}_t \sim q(\mathbf{x}_t|\mathbf{x}_0)$
      Forward Model $\epsilon_\theta(\mathbf{x}_t, \mathbf{c})$
      Compute Loss $L_{t-1}(\mathbf{x}, \mathbf{c}) = ||\epsilon_\theta(\mathbf{x}_t, \mathbf{c}) - \epsilon||_2^2$
      Compute Loss $\mathcal{L}_{\mathtt{DOM}}(\theta) = L_{t-1}(\mathbf{x}, \mathbf{c})$
      Backpropagate $\theta \leftarrow \nabla_\theta \mathcal{L}_{\mathtt{DOM}}(\theta)$
  end while
```

```python
import numpy as np
import torch as th

def compute_kernel_load(batch_load_sample, axis):

    size = batch_load_sample.size(-1)
    if axis == "x":
        ix = 0
        xx = th.argwhere(batch_load_sample[0] != 0)
        coord = xx
    elif axis == "y":
        ix = 1
        yy = th.argwhere(batch_load_sample[1] != 0)
        coord = yy

    if len(coord) == 0:
        return batch_load_sample[ix], []

    x_grid = th.tensor([i for i in range(size)])
    y_grid = th.tensor([j for j in range(size)])

    kernel_load = 0
    for l in range(len(coord)):
        x_grid = th.tensor([i for i in range(size)])
        y_grid = th.tensor([j for j in range(size)])
        # distance
        x_grid = x_grid - coord[l][0]
        y_grid = y_grid - coord[l][1]

        grid = th.meshgrid(x_grid, y_grid)

        r_load = th.sqrt(grid[0]**2 + grid[1]**2)

        if axis == "x":
            p = batch_load_sample[0][coord[l][0], coord[l][1]]
        elif axis == "y":
            p = batch_load_sample[1][coord[l][0], coord[l][1]]

        kernel = 1 - th.exp(- 1/r_load**2)
        kernel_load += kernel * p

    return kernel_load, coord
```

Listing 1: Dense Kernel Relaxation for Sparse Loads.

B Physics-based Conditioning on Constraints

Green's functions. To improve the efficiency of diffusion-based topology generation and minimize reliance on force and strain fields, we aim to relax boundary conditions and loads by leveraging kernels as approximations for the way such constraints act on the domain. One possible choice of kernel structure is inspired by Green's method [36, 34, 16, 41], which defines integral functions that are solutions to the time-invariant Poisson's Equation [33, 41], a generalization of Laplace's Equation for point sources excitations. Poisson's Equation can be written as $\nabla_x^2 f(x) = h$, where h is a forcing term and f is a generic function defined over the domain $\mathcal{X}$. This equation governs many phenomena in nature, and a special case is a forcing part $h = 0$, which yields the Laplace's Equation formulation commonly employed in heat transfer problems.

Green's method (or the Green's method family) is a mathematical construction to solve partial differential equations without prior knowledge of the domain. The solutions obtained with this method are known as Green's functions [53]. While solutions obtained with this method can be generally complex, for a large class of physical problems involving constraints and forces that can be approximated with points, a simple functional form can be derived by leveraging the idea of source and sink. Consider a laminar domain (e.g., a beam or a plate) constrained in a feasible way. If a point source is applied to this domain (e.g., a downward force on the edge of a beam or on the center of a plate) in x_f, such force can be described using the Dirac delta function, $\delta(x - x_f)$. The delta function is highly discontinuous but has powerful integration properties, in particular $\int f(x)\delta(x - x_f)dx = f(x_f)$ over the domain $\mathcal{X}$. The solution of the time-invariant Poisson's Equation with point concentrated forces can be written as a Green's function solution, where the solution depends only on the distance from the force application point. In particular:

$$\mathcal{G}(x, x') = -\frac{1}{4\pi}\frac{1}{|x - x'|}, \tag{9}$$

where $r = |x - x'| = \sqrt{|x_i - x_i'|^2 + |x_j - x_j'|^2}$. We propose to approximate the forces and loads applied to our topologies using a kernel relaxation built using Green's functions. While this formulation may not provide a correct solution for generic loads and boundary conditions, it allows us to provide computationally inexpensive conditioning information that respects the original physical and engineering constraints. By leveraging these ideas, we aim to increase the amount of information provided to condition the model, ultimately improving generative models with constraints.

Table 8: Design and Modelling requirements for a constrained generative model for topology optimization. Our goal is to improve the requirements that are challenging to fulfill. In this work, we focus on improving Floating Material, reducing Compliance Error, and reducing Sampling Time.

CLASS	METRICS	GOAL
Hard-constraint	Loads Disrespect	Feasibility
Hard-constraint	Floating Material	Manufacturability
Soft-constraint	Volume Fraction	Min Cost
Functional Performance	Compliance Error	Max Performance
Modeling Requirements	Sampling Time	Fast Inference

C Tables and Visualizations

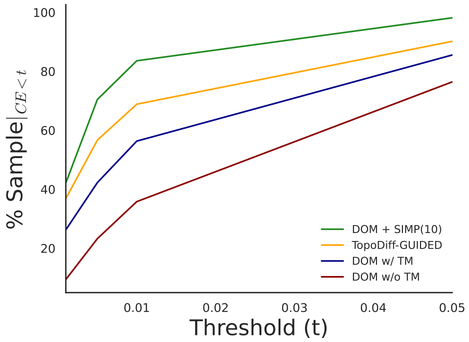

(a) Ratio of generated samples with CE $< t$.

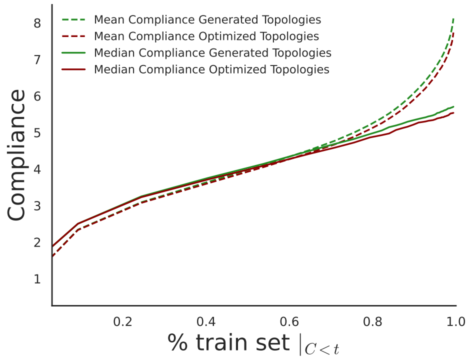

(b) Ratio of the training set with compliance $< t$.

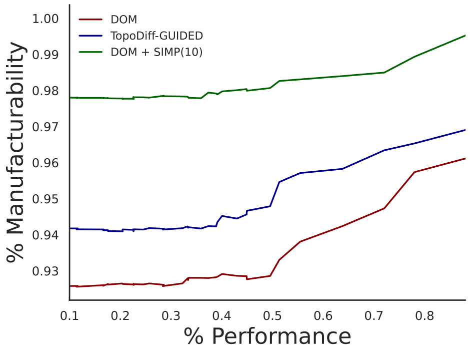

(c) Manufacturability vs Performance.

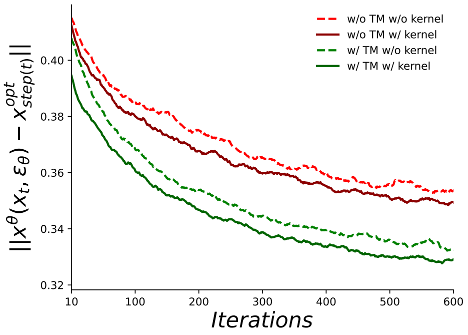

(d) Distance sampling and optimization path.

Table 9: Conditioning or guiding variables for different optimization methods and model configurations.

	Load	BC	Kernel Load	Kernel BC	Force Field	Energy Field	VF	Performance
SIMP [14]	✓	✓	✗	✗	✗	✗	✓	✓
TopologyGAN [69]	✓	✓	✗	✗	✓	✓	✓	✗
TopoDiff [62]	✓	✓	✗	✗	✓	✓	✓	✓
TopoDiff-FF [37]	✓	✓	✓	✓	✗	✗	✓	✗
DOM (ours)	✓	✓	✓	✓	✗	✗	✓	✗
DOM + Trajectory Alignment (ours)	✓	✓	✓	✓	✗	✗	✓	✓
DOM + Optimizer (ours)	✓	✓	✓	✓	✗	✗	✓	✓

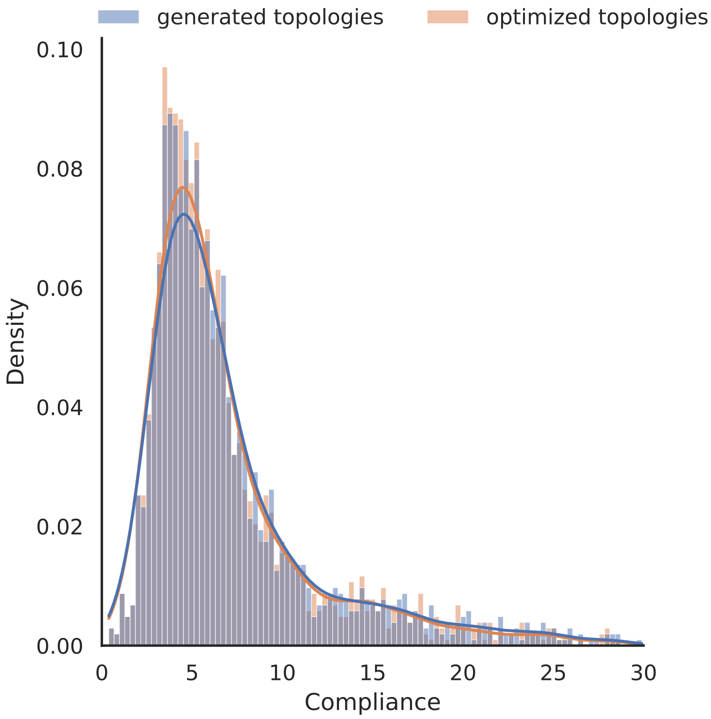

Figure 8: Histogram empirical distribution compliance for generated and optimized topologies.

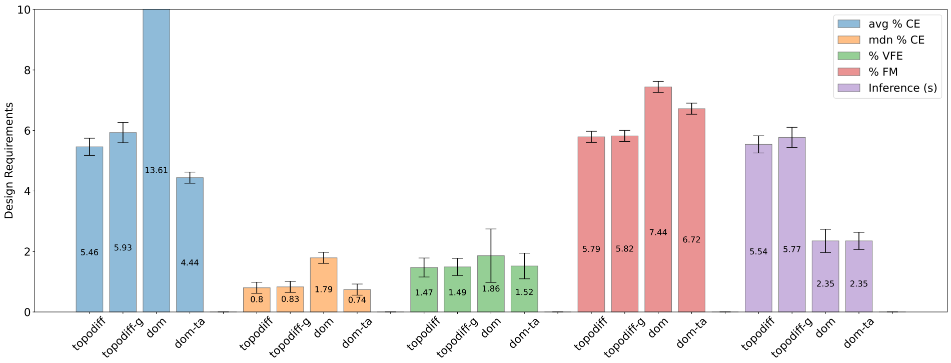

Figure 9: Confidence interval for design requirements on in-distribution constraint configurations.

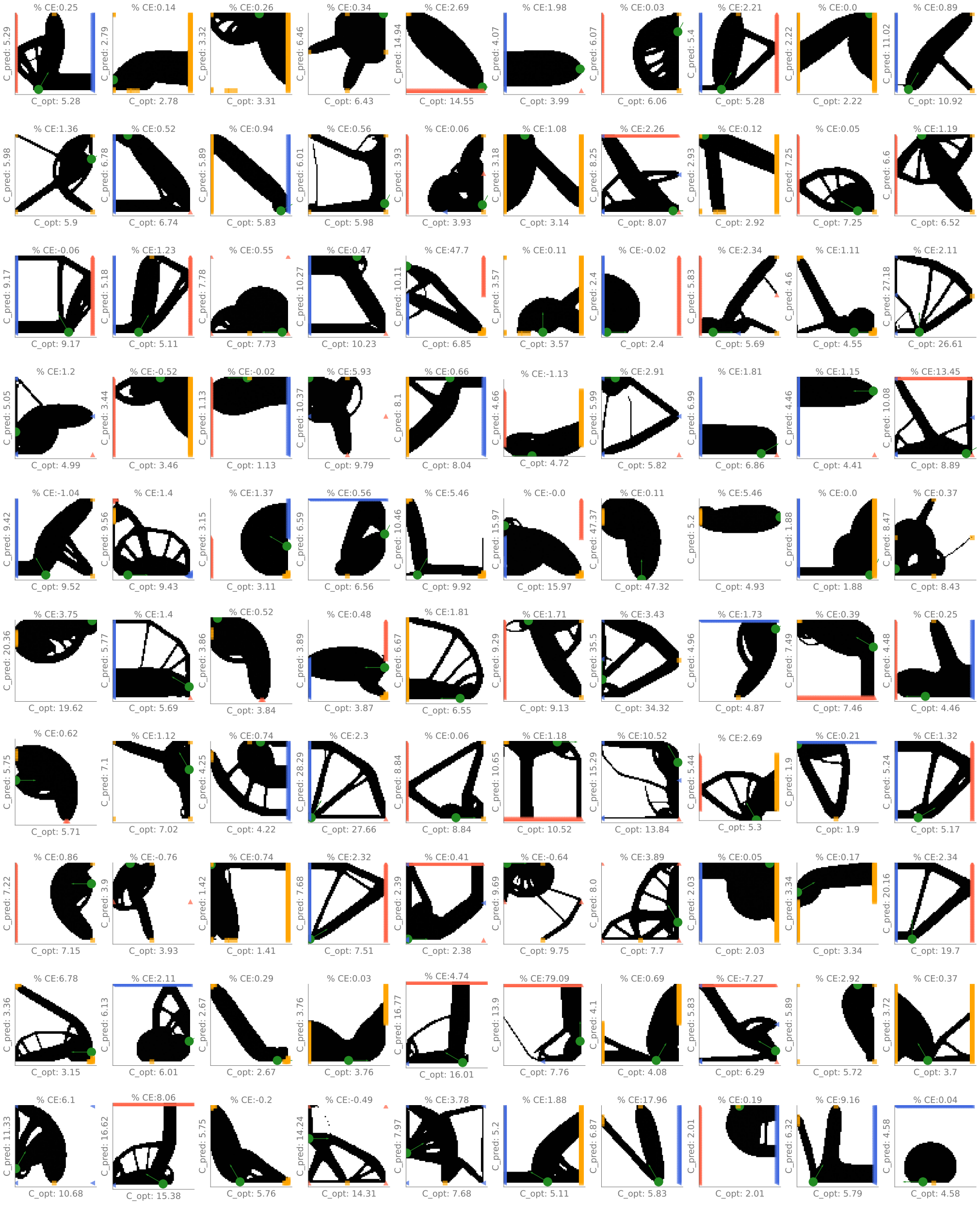

Figure 10: Examples of generated topologies with good performance.

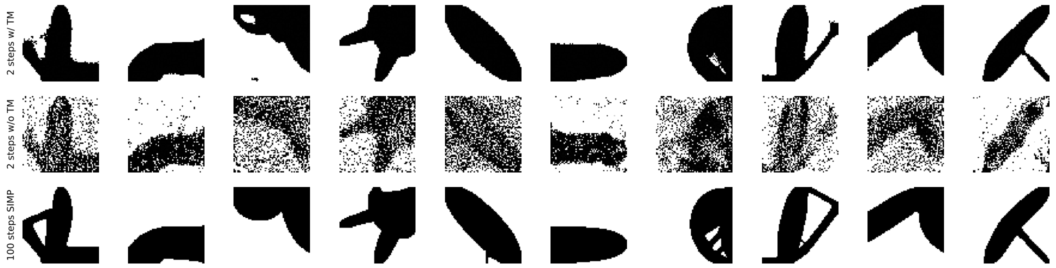

Figure 11: Comparison DOM w/ TA and DOM w/o TA generation with 2 steps.

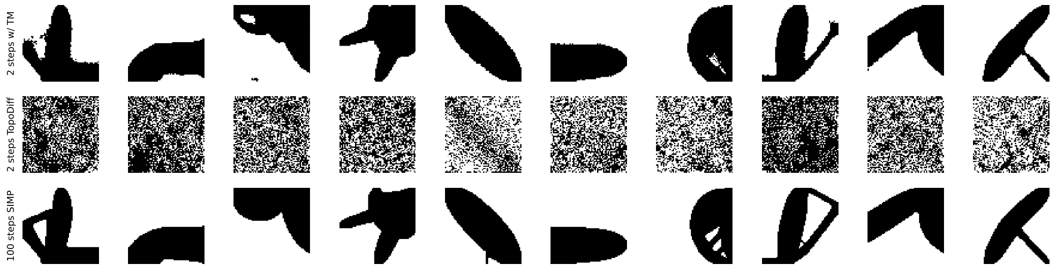

Figure 12: Comparison DOM w/ TA and TopoDiff-GUIDED generation with 2 steps.

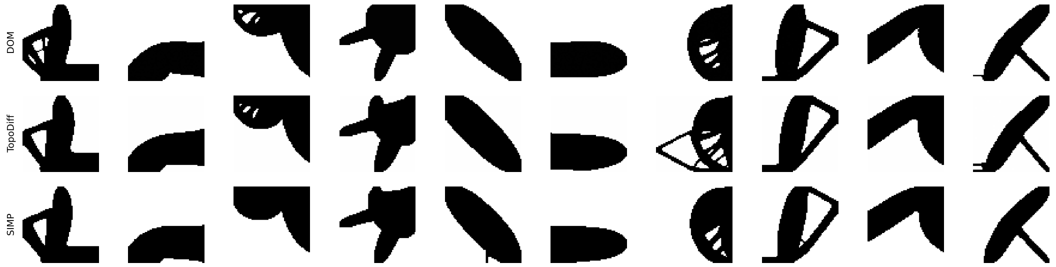

Figure 13: Comparison DOM and TopoDiff-GUIDED generation with 100 steps.

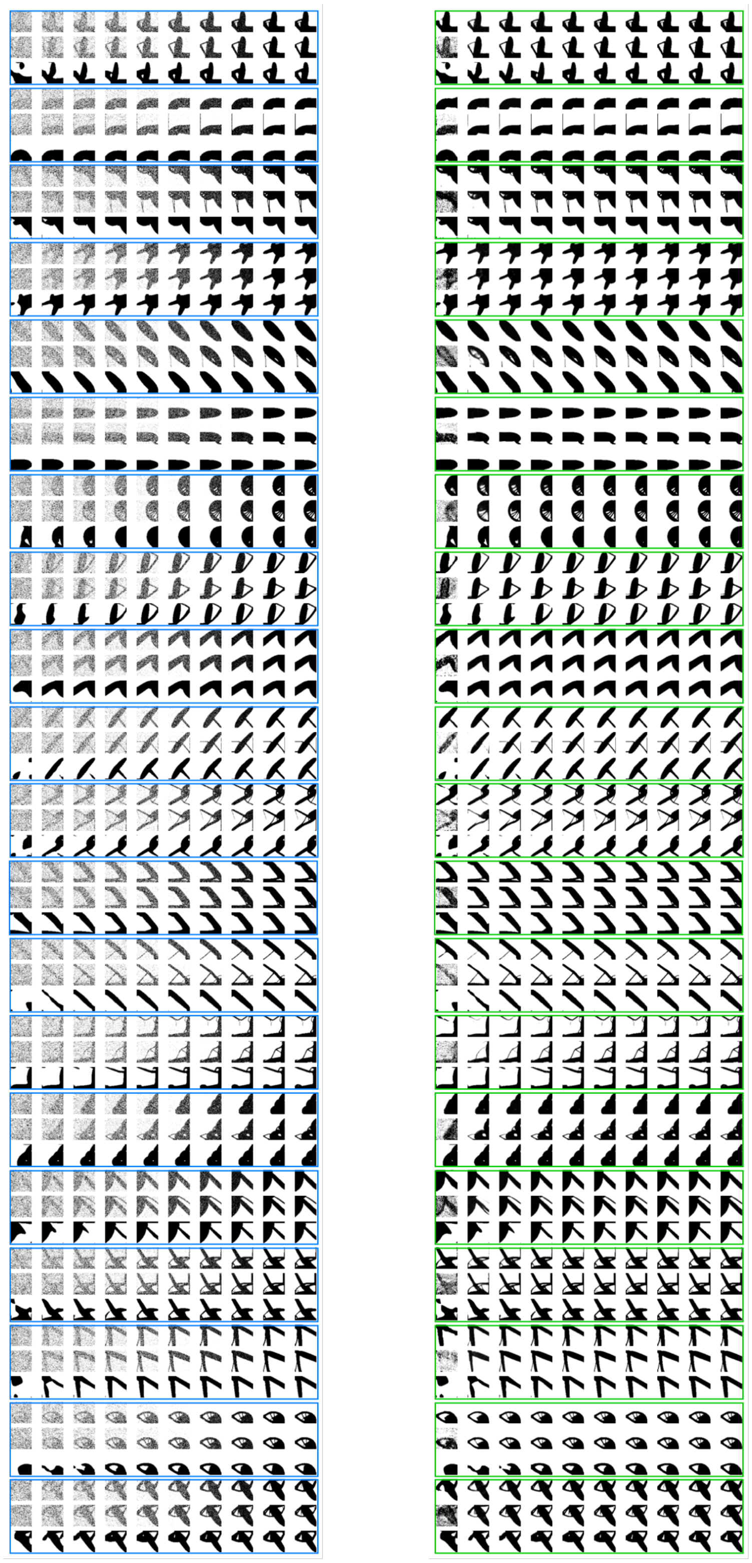

Figure 14: Left: $\mathbf{x}_t^{\theta}$ from 10 intermediate generation steps for DOM w/ TA (top block), DOM w/o TA (middle block), SIMP iterations (bottom block). Right: Prediction of $\tilde{\mathbf{x}}^{\theta}$ from 10 intermediate generation steps for DOM w/ TA (top block), DOM w/o TA (middle block), SIMP iterations (bottom block).

D Dataset

We build a dataset of optimized topologies and intermediate optimization steps at low-resolution (64x64) and high-resolution (256x256). In particular:

- 50K low-resolution optimized topologies w/ constraints.
- 60K high-resolution optimizer topologies w/ constraints.
- 250K low-resolution intermediate steps [10, 20, 30, 50, 70] w/ constraints.
- 300K high-resolution intermediate steps [10, 20, 30, 50, 70] w/ constraints.

In Figure 15, 16, 17, 18 we show examples of intermediate steps at 10, 20, 30, and optimized topologies at high-resolution.

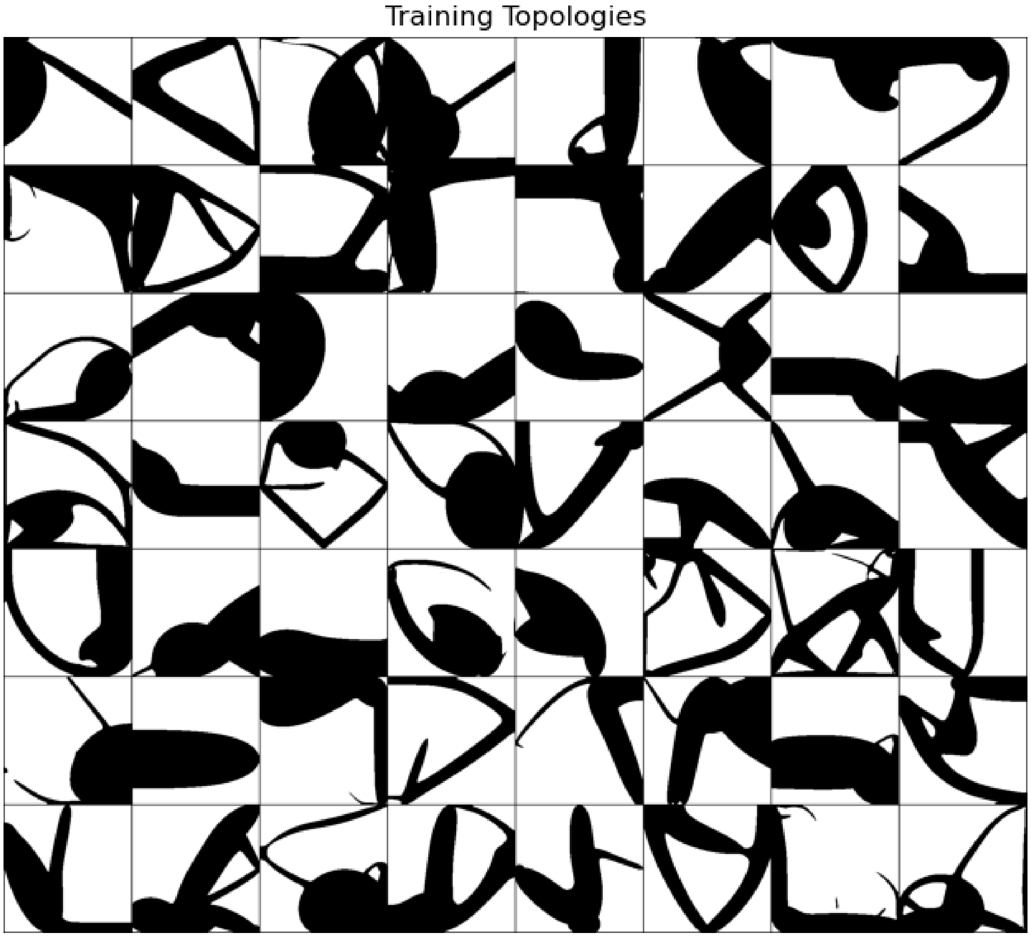

Figure 15: Intermediate optimization output after 10 iterations. Resolution: 256x256.

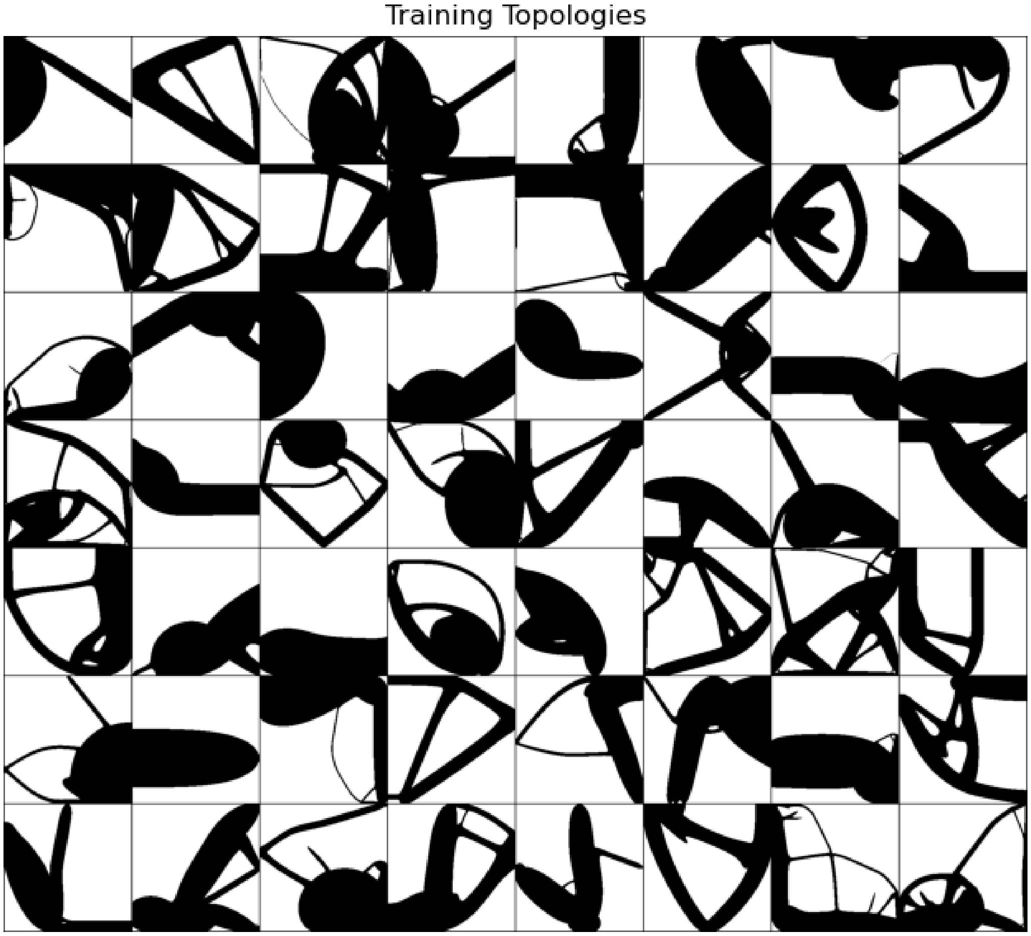

Figure 16: Intermediate optimization output after 20 iterations. Resolution: 256x256.

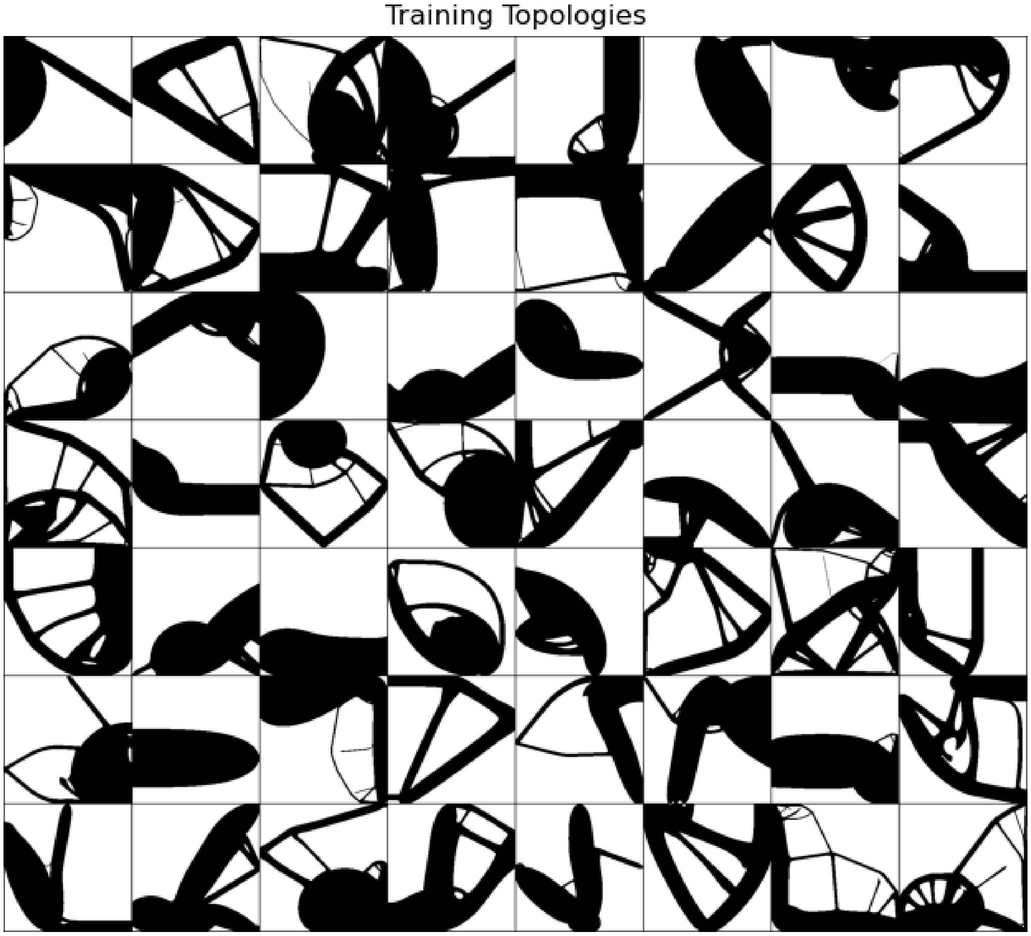

Figure 17: Intermediate optimization output after 30 iterations. Resolution: 256x256.

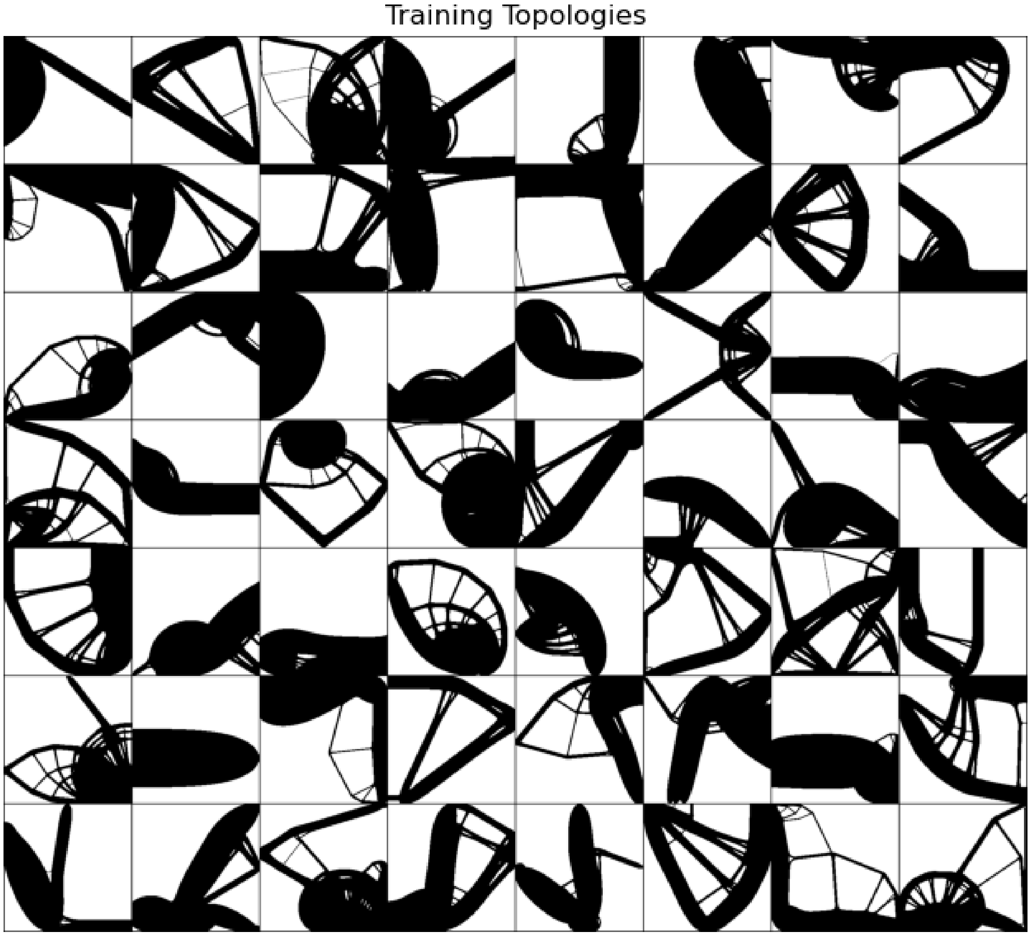

Figure 18: Optimized output. Resolution: 256x256.

E Experimental Details

Table 10: Relevant Hyperparameters for baselines and DOM on 64x64 datasets.

	TopoDiff	TopoDiff-G	DOM w/o TA	DOM w/ TA
Dimension	1x64x64	1x64x64	1x64x64	1x64x64
Model Set	30k	30K	30K	30K
Guidance Set	-	150K	-	-
Intermediate Set	-	-	-	150K
Test Configurations	1800	1800	1800	1800
Batch size	64	64	64	64
Architecture	Unet	Unet	Unet	Unet
Iterations	200K	200K	200K	200K
Learning rate	$2e^{-4}$	$2e^{-4}$	$2e^{-4}$	$2e^{-4}$
Loss	L_ϵ	L_ϵ	L_ϵ	$L_\epsilon + L_{\texttt{TA}}$
Optimizer	Adam	Adam	Adam	Adam